C–C bond in **9**, which prevents direct isomerization of **9** into **8** (eq 7), might be rationalized by assuming that dissociation of one of the imine nitrogen bonds from a ruthenium center in this complex is a process requiring less energy than fission of the central C–C bond and takes place reversibly when **9** is heated or irradiated. Invoking the formation of an unsaturated 16e ruthenium center also accounts for the photochemical acceleration of the uptake of a CO ligand by **9** to give **7** (reverse of eq 5).

Comparison with Reactions in the $Ru_3(CO)_{12}$/R-Pyca System. The reactions within the $Ru_m(CO)_n$/R-DAB system (Scheme I) roughly parallel those in the $Ru_3(CO)_{12}$/R-Pyca system [R-Pyca = 6-R′C_5H_3N-2-(C(H)=NR)].[2,44] In the R-Pyca case $Ru_2(CO)_4$(R-Pyca)$_2$, a complex isostructural to **8**, proved to be formed directly from $Ru_2(CO)_5$(R-APE) or from $Ru_2(CO)_6$(R-Pyca) and R-Pyca without the intermediacy of $Ru_2(CO)_4$(R-APE). This sequence also appears to be valid in the R-DAB system. Some important differences between the two systems, however, should be noted. First, $Ru(CO)_3$(R-Pyca) neither is formed during reactions of $Ru_2(CO)_4$(R-Pyca)$_2$ or $Ru_2(CO)_5$(R-APE) with CO nor has been observed as a product (or intermediate) during thermal reactions of $Ru_3(CO)_{12}$ with R-Pyca.[44] This suggests that under the applied reaction conditions $Ru(CO)_3$(R-Pyca) is even more labile than $Ru(CO)_3$(R-DAB) (**6**) with respect to CO elimination. This is in line with the observation that no formation of $Ru(CO)_3$(R-Pyca) occurs during reactions of $Ru(CO)_5$ with R-Pyca.[48] Second, the reactivity of $Ru_2(CO)_5$(R-APE) depends mainly on the substituents on the 6-positions of the pyridyl parts of the R-APE ligand and, in contrast to the corresponding R-ADA compounds, only little on the reaction temperature or the R groups on the N atoms. For the R-Pyca derivatives $Ru_2(CO)_4$(R-APE) was formed only when a methyl group was present in the 6-position. With an H atom at this position $Ru_2(CO)_4$(R-Pyca)$_2$ was the main product.

Conclusions

We have shown that, provided the correct kinetic reaction path is chosen, $Ru(CO)_3$(R-DAB) (R = *i*-Pr (**6a**), c-Hex (**6b**), *p*-Tol (**6d**)) can be obtained as a pure compound in solution, applying reversible thermal carbonylation reactions of the known complexes $Ru_2(CO)_5$(R-ADA) (**7a,b**) or $Ru_2(CO)_4$(*p*-Tol-DAB)$_2$ (**8d**). The intermediacy of complex I with stoichiometry $Ru_2(CO)_5$(R-DAB)$_2$, which could be observed in a low steady-state concentration by irradiating a solution of **6a** at low temperature (−70 °C), is proposed. The present study has provided a more detailed insight into the thermally and photochemically induced interconversions between R-DAB and R-ADA complexes in the $Ru_m(CO)_n$/R-DAB system and the crucial role of CO therein.

Acknowledgment. We thank Prof. G. van Koten for his interest, D. Heijdenrijk for collecting the X-ray data, M. van Wijnkoop and M. J. A. Kraakman for helpful discussions, G. U. A. Sai and R. Fokkens of the Instituut voor Massa Spectrometrie, Universiteit van Amsterdam, for recording the mass spectra, and J. M. Ernsting for recording the 62.9-MHz ^{13}C NMR spectra. Furthermore, we thank G. C. Schoemaker and A. Terpstra for their assistance during the low-temperature photolysis experiments. The research was supported by the Netherlands Foundation for Chemical Research (SON) with financial aid from the Netherlands Organization for Scientific Research (NWO).

Supplementary Material Available: Tables of complete crystal structure data, all bond lengths and angles, anisotropic thermal parameters of the non-hydrogen atoms, and calculated fractional coordinates and the isotropic thermal parameters of the H atoms (8 pages); a listing of the structure factor amplitudes (13 pages). Ordering information is given on any current masthead page.

---

(48) $Ru(CO)_5$ (ca. 0.2 mmol) and *i*-Pr-Pyca (4 mmol) in hexane were stirred at room temperature for 6 h. During this period the IR frequencies belonging to $Ru(CO)_5$ (2037 and 2002 cm^{-1}) gradually disappeared and a dark blue precipitate was formed. This product, which is insoluble in common organic solvents (dichloromethane, ether, hexane, THF), is not air sensitive and shows three broad IR frequencies in KBr (2033 (w), 1970 (s), 1902 (w) cm^{-1}). These observations clearly indicate that this product is not $Ru(CO)_3$(*i*-Pr-Pyca).

Contribution from Crystalytics Company, Lincoln, Nebraska 68501, and Departments of Chemistry, University of Nebraska, Lincoln, Nebraska 68588, and University of Illinois, Urbana, Illinois 61801

$Nb_2W_4O_{19}^{4-}$ and $P_3O_9^{3-}$ Complexes of (Cyclooctadiene)iridium(I): Synthesis, Structure, and Stability of Tetra-*n*-butylammonium Salts of $\{[(C_8H_{12})Ir]_5(Nb_2W_4O_{19})_2\}^{3-}$, $\{[(C_8H_{12})Ir]_2H(Nb_2W_4O_{19})_2\}^{5-}$, and $[(C_8H_{12})Ir(P_3O_9)]^{2-}$

V. W. Day,*,† W. G. Klemperer,*,‡ and D. J. Main‡

Received July 28, 1989

Stoichiometric reaction of $[(C_8H_{12})Ir(NCCH_3)_2]PF_6$ with $Nb_2W_4O_{19}[(n\text{-}C_4H_9)_4N]_4$ in CH_2Cl_2 yields crystalline $\{[(C_8H_{12})Ir]_5(Nb_2W_4O_{19})_2\}[(n\text{-}C_4H_9)_4N]_3$ (**1**). IR and $^{13}C\{^1H\}$ NMR spectroscopy indicate that the anion of **1** is isostructural with the (norbornadiene)rhodium(I) complex $\{[(C_7H_8)Rh]_5(Nb_2W_4O_{19})_2\}^{3-}$ (anion of **2**) and contains two octahedral $Nb_2W_4O_{19}^{4-}$ ions linked together in a face-to-face fashion by five four-coordinate $(C_8H_{12})Ir^+$ units. Reaction of compound **1** with $Nb_2W_4O_{19}[(n\text{-}C_4H_9)_4N]_4$ and CH_3COOH in CH_3CN yields $\{[(C_8H_{12})Ir]_2H(Nb_2W_4O_{19})_2\}[(n\text{-}C_4H_9)_4N]_5$ (**3**) [a = 16.618 (4) Å, b = 16.548 (4) Å, c = 30.729 (6) Å, α = 87.02 (2)°, β = 94.57 (2)°, γ = 114.20 (2)°, triclinic; $P\bar{1}\text{-}C_i^1$; Z = 2]. According to single-crystal diffraction and ^{17}O NMR spectroscopic studies, the anion of **3** contains two $Nb_2W_4O_{19}^{4-}$ ions linked together in an edge-to-edge fashion by two four-coordinate $(C_8H_{12})Ir^+$ units and one proton. The trimetaphosphate complex $[(C_8H_{12})Ir(P_3O_9)][(n\text{-}C_4H_9)_4N]_2$ **4** [a = 11.324 (2) Å, b = 13.288 (2) Å, c = 34.035 (5) Å, β = 101.24 (1)°, monoclinic; $P2_1/c\text{-}C_{2h}^5$; Z = 4] is prepared from $[(C_8H_{12})Ir(NCCH_3)_2]PF_6$ and $P_3O_9[(n\text{-}C_4H_9)_4N]_3$. A single-crystal X-ray diffraction study of compound **4** revealed the presence of discrete $[(C_8H_{12})Ir(P_3O_9)]^{2-}$ anions in which the iridium center is square-pyramidally coordinated, with the two cyclooctadiene olefinic units occupying basal sites and three trimetaphosphate oxygens spanning the remaining basal and apical sites. Addition of 250 equiv of CD_3CN/equiv of Ir to CD_3NO_2 solutions of **1**, **3**, and **4**, all 3.5 mM in Ir, completely decomposes the anion of **1**, partially decomposes the anion of **3**, but leaves the anion of **4** intact, according to ^1H NMR spectroscopic data.

Organorhodium(I) and organoiridium(I) complexes are known to have an extensive reaction chemistry in fluid solution and on solid oxide supports.[1] In order to combine key features associated with solution and solid-state environments, reactions of these complexes with both main-group and transition-metal polyoxoanions have been investigated.[2-5] Two polyoxoanion-supported

---

† Crystalytics Co. and University of Nebraska.
‡ University of Illinois.

(1) Dickson, R. S. *Homogeneous Catalysts with Compounds of Rhodium and Iridium*; Reidel: Boston, MA, 1985.

0020-1669/90/1329-2345$02.50/0

organorhodium(I) complexes have been isolated and structurally characterized, the (norbornadiene)rhodium(I) complexes $\{[(C_7H_8)Rh]_5(Nb_2W_4O_{19})_2\}^{3-}$[2a] and $[(C_7H_8)Rh(P_3O_9)]^{2-}$.[2b] Here the synthesis, structure, and relative stabilities of three related (cyclooctadiene)iridium(I) complexes are described that involve the same polyoxoanion ligands. The reactivity of these complexes toward carbon monoxide and oxygen will be treated in future publications.[6]

Experimental Section

Reagents, Solvents, and General Procedures. The following were purchased from commercial sources and used without further purification: $AgPF_6$ (Aldrich), glacial acetic acid (Baker), $(NH_4)_2IrCl_6$ (Aesar), and ^{17}O-enriched water (Monsanto).

$[(C_8H_{12})IrCl]_2$,[7] $Nb_2W_4O_{19}[(n\text{-}C_4H_9)_4N]_4$,[8] $[(C_7H_8)Rh(NCCH_3)_2]PF_6$,[2b] $P_3O_9[(n\text{-}C_4H_9)_4N]_3\cdot 2.5H_2O$,[2b] and $[(C_7H_8)Rh(P_3O_9)][(n\text{-}C_4H_9)_4N]_2$[2b] were prepared by using published procedures. $(C_8H_{12})Ir(C_5H_7O_2)$, $C_5H_7O_2$ = acetylacetonate, was prepared according to ref 9, method 1, by using $[(C_8H_{12})IrCl]_2$ as the iridium-containing starting material. Oxygen-17 enrichment of $Nb_2W_4O_{19}[(n\text{-}C_4H_9)_4N]_4$ was accomplished with the method described in ref 8.

Acetonitrile (Aldrich), methylene chloride, chloroform, nitromethane-d_3 (all Fisher), and 1,2-dichloroethane (Baker) were distilled from P_4O_{10} under N_2. Nitrobenzene-d_5 (Aldrich) was vacuum-distilled from BaO (Fisher). Acetone (Fisher) was distilled from dehydrated boron oxide (Aldrich) under N_2. Ether (Mallinckrodt) and toluene (Fisher) were distilled from sodium benzophenone ketyl under N_2. All solvents (except acetone) were stored over 3-Å molecular sieves (Linde). Molecular sieves were activated by heating at 350 °C for 24 h and cooling under vacuum.

Reactions involving iridium and rhodium reagents were routinely performed in a N_2 atmosphere. All manipulations of ^{17}O-enriched materials were performed in closed systems with rigorous exclusion of moisture to avoid isotopic dilution.

Analytical Procedures. Elemental analyses were performed by the School of Chemical Sciences analytical laboratory and by Galbraith Laboratories, Knoxville, TN. Infrared spectra were measured from mineral oil (Nujol) mulls between KBr plates on a Perkin-Elmer Model 1330 infrared spectrophotometer and were referenced to the 1028-cm^{-1} band of 0.05-mm polystyrene film.

^1H and $^{13}C\{^1H\}$ NMR spectra were recorded either at 360 and 90.5 MHz, respectively, on a Nicolet NTC-360 spectrometer or at 300 and 75.5 MHz, respectively, on a General Electric QE-300 spectrometer. Chemical shifts were internally referenced to tetramethylsilane. Most of the compounds examined were $(n\text{-}C_4H_9)_4N^+$ salts, and the ^1H and $^{13}C\{^1H\}$ NMR resonances arising from this cation are not listed below. These resonances appeared as multiplets centered at about δ 3.2, 1.7, 1.4, and 1.0 in ^1H NMR spectra and as singlets at about δ 59, 25, 21, and 14 in $^{13}C\{^1H\}$ NMR spectra.

$^{31}P\{^1H\}$ NMR spectra were recorded at 101.3 MHz in 12-mm-o.d. vertical sample tubes on an unlocked FTNMR system equipped with a 5.87-T Oxford Instruments magnet and a Nicolet NIC-1280 data processor. The magnet was shimmed by tuning the probe to deuterium and observing the deuterated solvent signal. All spectra were externally referenced to 85% H_3PO_4 by the sample replacement method.

^{17}O NMR spectra were measured at 33.9 MHz in 12-mm-o.d. vertical sample tubes without sample spinning on an unlocked FTNMR system equipped with a 5.87-T Oxford Instruments magnet and a Nicolet NIC-1280 data processor. The magnet was shimmed by tuning the probe to ^{133}Cs and observing an aqueous CsI sample. All spectra were externally referenced to 22 °C fresh tap water by the sample replacement method. Chemical shifts are reported as positive numbers for resonances observed at high frequency (low field) relative to the reference frequency. The pulse repetition rate was 5.88 Hz, spectral bandwidth 40 kHz, pulse width 27 μs, preacquisition delay 25 μs, and digitization (frequency domain) 8192. To improve the signal-to-noise ratio, 15-Hz exponential line broadening was employed; all reported line widths have been corrected for this.

Preparation of $[(C_8H_{12})Ir(NCCH_3)_2]PF_6$. To a solution containing 2.02 g (3.01 mmol) of $[(C_8H_{12})IrCl]_2$ in 42 mL of CH_2Cl_2 was added 10 mL of CH_3CN. The solution changed color from dark red to bright yellow, and 1.52 g (6.01 mmol) of $AgPF_6$ was added causing AgCl to precipitate. The solution was filtered into 200 mL of diethyl ether, and after a few minutes yellow microcrystals precipitated. These were collected by suction filtration, washed with 2 × 10 mL of diethyl ether, and dried under vacuum for 12 h (2.56 g, 4.85 mmol, 81% yield). ^1H NMR[10] (360 MHz, CD_2Cl_2, 22 °C): δ 4.27 (s, CH), 2.53 (s, CH_3), 2.29 (m, CH_2), 1.78 (m, CH_2). $^{13}C\{^1H\}$ NMR (90.5 MHz, CD_3NO_2, 22 °C): δ 125.3 (s, CN), 72.9 (s, CH), 32.1 (s, CH_2), 3.2 (t, CH_3).

Preparation of $\{[(C_8H_{12})Ir]_5(Nb_2W_4O_{19})_2\}[(n\text{-}C_4H_9)_4N]_3$ (1). A solution of 2.76 g (1.26 mmol) of $Nb_2W_4O_{19}[(n\text{-}C_4H_9)_4]_4$ in 7 mL of CH_2Cl_2 was added dropwise with stirring to a solution of 1.66 g (3.15 mmol) of $[(C_8H_{12})Ir(NCCH_3)_2]PF_6$ in 5 mL of CH_2Cl_2 over a period of 2 min. During this addition, the product began to precipitate from solution as an orange microcrystalline solid. Stirring was continued for 10 min after the addition was complete, and the crystals were collected by suction filtration, washed with 2 × 5 mL of $CHCl_3$ and 2 × 5 mL of diethyl ether, and dried in vacuo for 24 h (2.4 g, 0.51 mmol, 81%). Anal. Calcd for $C_{88}H_{168}N_3Ir_5Nb_4W_8O_{38}$: C, 22.59; H, 3.62; N, 0.90; Ir, 20.54; Nb, 7.94; W, 31.43. Found: C, 22.51; H, 3.61; N, 0.89; Ir, 20.39; Nb, 8.22; W, 31.48. IR (Nujol, 650–1000 cm^{-1}): 740 (s, br), 795 (s, br), 835 (s), 913 (m), 966 (s) cm^{-1}. ^1H NMR (360 MHz, CD_3NO_2, 22 °C): δ 5.3, 5.2, 4.1, 2.4, 2.3, 2.1. $^{13}C\{^1H\}$ NMR (90.5 MHz, $C_6D_5NO_2$, 22 °C): δ 60.2 (s, CH), 60.1 (s, CH), 59.7 (s, CH), 58.3 (s, CH), 58.1 (s, CH), 33.3 (s, CH_2), 33.1 (s, CH_2), 32.5 (s, CH_2), 32.1 (s, CH_2).

Recrystallization could be accomplished by dissolving the product in 36 mL of boiling CH_3NO_2, gravity filtering the mixture, and letting the solution cool to room temperature. The red-orange needles that precipitated were collected by suction filtration, washed with 2 × 5 mL of diethyl ether, and dried under vacuum for 12 h (1.1 g, 0.24 mmol, 46%).

Preparation of $\{[(C_7H_8)Rh]_5(Nb_2W_4O_{19})_2\}[(n\text{-}C_4H_9)_4N]_3$ (2). A solution of 0.31 g (0.14 mmol) of $Nb_2W_4O_{19}[(n\text{-}C_4H_9)_4N]_4$ in 1 mL of CH_2Cl_2 was added dropwise to a stirred solution of 0.15 g (0.36 mmol) of $[(C_7H_8)Rh(NCCH_3)_2]PF_6$ in 1 mL of CH_2Cl_2 over a period of 2 min. The orange microcrystalline product that slowly precipitated from the orange reaction solution was collected by suction filtration, washed with 2 × 1 mL of CH_2Cl_2 and 2 × 5 mL of diethyl ether, and dried under vacuum for 24 h (0.20 g, 0.05 mmol, 71% based on W). IR (Nujol, 650–1000 cm^{-1}): 756 (s, br), 791 (s), 811 (s), 833 (s), 912 (m), 962 (s) cm^{-1}. See ref 2a for elemental analysis and $^{13}C\{^1H\}$ NMR data.

Preparation of $\{[(C_8H_{12})Ir]_2H(Nb_2W_4O_{19})_2\}[(n\text{-}C_4H_9)_4N]_5$ (3). To a suspension of 0.47 g (0.11 mmol) of $\{[(C_8H_{12})Ir]_5(Nb_2W_4O_{19})_2\}[(n\text{-}C_4H_9)_4N]_3$ in 4 mL of CH_3CN was added 0.66 g (0.30 mmol) of $Nb_2W_4O_{19}[(n\text{-}C_4H_9)_4N]_4$. The resulting cloudy orange solution was stirred for 2 h, after which time 16.2 μL (0.28 mmol) of CH_3COOH was added. The slightly cloudy orange solution was then filtered via cannula into 150 mL of ether with rapid stirring, causing an oily yellow solid to precipitate. This solid was washed with 20 mL of diethyl ether and dried under vacuum for 24 h (0.94 g, 0.22 mmol, 85% based on W). Crystallization was accomplished by dissolving the crude product in 3.6 mL of 1,2-dichloroethane, filtering the mixture through cotton, and slowly adding to the filtrate 1.5 mL of toluene followed by 12 μL (0.21 mmol) of CH_3COOH. The bright yellow crystals that precipitated within 30 min were washed with 20 mL of diethyl ether and dried under vacuum for 24 h (0.53 g, 0.12 mmol, 46% overall yield based on W). The analytical sample was crystallized a second time by following the same procedure but omitting the acetic acid. Anal. Calcd for $C_{96}H_{205}N_5Ir_2Nb_4W_8O_{38}$: C, 27.04; H, 4.85; N, 1.64; Ir, 9.01; Nb, 8.71; W, 34.49. Found: C, 27.06; H, 4.74; N, 1.69; Ir, 9.12; Nb, 8.63; W, 34.64. IR (Nujol, 650–1000 cm^{-1}): 771 (s, br), 805 (s, sh), 900 (m), 952 (s) cm^{-1}. ^1H NMR (360 MHz, CD_3NO_2, 22 °C): δ 3.9 (br, CH), 2.2 (br, CH_2), 1.4 (q, CH_2). $^{13}C\{^1H\}$ NMR (90.5 MHz, CD_3NO_2, 22 °C): δ 58.5 (s, CH), 32.8 (s, CH_2). ^{17}O NMR (33.9 MHz, 14 mM in CH_3NO_2, 20 °C, $\leq$10 atom % ^{17}O, 258 800 acquisitions): δ 727 (571 Hz

---

(2) (a) Besecker, C. J.; Klemperer, W. G.; Day, V. W. *J. Am. Chem. Soc.* **1982**, *104*, 6158. (b) Besecker, C. J.; Day, V. W.; Klemperer, W. G. *Organometallics* **1985**, *3*, 564. (c) Klemperer, W. G.; Yagasaki, A. *Chem. Lett.* **1989**, 2041.

(3) Finke, R. G.; Edlund, D. J.; Lyon, D. K. *Abstracts of Papers*, Third Chemical Congress of North America, Toronto, Canada; American Chemical Society: Washington, DC, 1988; INOR 426.

(4) Urabe, K.; Tanaka, Y.; Izumi, Y. *Chem. Lett.* **1985**, 1595.

(5) (a) Siedle, A. R.; Markell, C. G.; Lyon, P. A.; Hodgson, K. O.; Roe, A. L. *Inorg. Chem.* **1987**, *26*, 219. (b) Siedle, A. R.; Newmark, R. A.; Brown-Wensley, K. A.; Skarjune, R. P.; Haddad, L. C.; Hodgson, K. O.; Roe, A. L. *Organometallics* **1988**, *7*, 2078. (c) Siedle, A. R.; Newmark, R. A.; Gleason, W. B.; Skarjune, R. P.; Hodgson, K. O.; Roe, A. L.; Day, V. W. *Solid State Ionics* **1988**, *26*, 109. (d) Siedle, A. R.; Newmark, R. A. *J. Am. Chem. Soc.* **1989**, *111*, 2058.

(6) (a) Klemperer, W. G.; Main, D. J. *Inorg. Chem.*, following paper in this issue. (b) Day, V. W.; Klemperer, W. G.; Lockledge, S. P.; Main, D. J. *J. Am. Chem. Soc.* **1990**, *112*, 2031.

(7) Crabtree, R. H.; Quirk, J. M.; Felkin, H.; Fillebeen-Khan, T. *Synth. React. Inorg. Met.-Org. Chem.* **1982**, *12*, 407.

(8) Besecker, C. J.; Day, V. W.; Klemperer, W. G.; Thompson, M. R. *J. Am. Chem. Soc.* **1984**, *106*, 4125.

(9) Robinson, S. D.; Shaw, B. L. *J. Chem. Soc.* **1965**, 4997.

(10) Green, M.; Kuc, T. A.; Taylor, S. H. *J. Chem. Soc. A* **1971**, 2334.

line width, OW), 520 (207 Hz, ONbIr), 457 (148 Hz, ONbW), 388 (343 Hz, OW_2), 293 (1230 Hz, ONb_2H).

Preparation of $[(C_8H_{12})Ir(P_3O_9)][(n\text{-}C_4H_9)_4N]_2$ (4). A solution of 0.60 g (1.1 mmol) of $[(C_8H_{12})Ir(NCCH_3)_2]PF_6$ in 2.0 mL of CH_2Cl_2 was added dropwise to a stirred solution of 1.10 g (1.09 mmol) of $P_3O_9[(n\text{-}C_4H_9)_4N]_3{\cdot}2.5H_2O$ in 2 mL of CH_2Cl_2 over a period of 2 min. After the green solution was stirred for 30 min, 10 mL of diethyl ether was added to precipitate the product as a green oil. The oil was washed with 2 × 10 mL of diethyl ether causing it to solidify to a light green powder, which was collected by suction filtration and dried under vacuum for 24 h (1.4 g, 1.37 mmol, 126%). The crude product was shown to contain PF_6^- by infrared spectroscopy [ν(P–F) = 557 cm^{-1}]. Crystallization was accomplished by dissolving the crude product in 2–3 mL of hot acetone, filtering the mixture through cotton, and slowly adding diethyl ether to the warm solution just until crystals began precipitating. The solution was cooled to room temperature, and after 1 h beautiful, rod-shaped, slightly hygroscopic, green crystals were collected on a medium frit, washed with 2 × 5 mL of diethyl ether, and dried under vacuum for 24 h (0.79 g, 0.77 mmol, 71% based on P). Anal. Calcd for $C_{40}H_{84}N_2IrP_3O_9$: C, 47.00; H, 8.28; N, 2.74; Ir, 18.80; P, 9.09. Found: C, 46.92; H, 8.30; N, 2.67; Ir, 18.88; P, 9.05. IR (Nujol, 650–1320 cm^{-1}): 740 (m), 776 (m), 793 (m, sh, br), 958 (s), 983 (m, sh), 1070 (m), 1130 (s), 1258 (s), 1268 (s), 1291 (s) cm^{-1}. ^1H NMR (300 MHz, CD_2Cl_2, 22 °C): δ 3.6 (m, CH), 2.1 (m, CH_2), 1.2 (q, CH_2). ^1H NMR (360 MHz, CD_3NO_2, 22 °C): δ 3.7 (m, CH), 2.2 (m, CH_2), 1.3 (q, CH_2). $^{13}C\{^1H\}$ NMR (75.5 MHz, CD_2Cl_2, 22 °C): δ 55.5 (s, CH), 31.1 (s, CH_2). $^{13}C\{^1H\}$ NMR (90.5 MHz, $C_6D_5NO_2$, 22 °C): δ 55.8 (s, CH), 32.2 (s, CH_2). $^{31}P\{^1H\}$ NMR (CD_2Cl_2): δ −12.0 (20 °C); δ −12.1 (−75 °C). $^{31}P\{^1H\}$ NMR (CD_3NO_2, 22 °C): δ −11.0.

Crossover Experiment. $^{31}P\{^1H\}$ NMR spectra of $\{[(C_8H_{12})Ir](P_3O_9)\}[(n\text{-}C_4H_9)_4N]_2$ (4) and $\{[(C_7H_8)Rh](P_3O_9)\}[(n\text{-}C_4H_9)_4N]_2$ (0.03 M in CD_3NO_2, 22 °C) were observed at δ −11.0 and −11.9, respectively. The two solutions were then mixed via syringe, and a $^{31}P\{^1H\}$ NMR spectrum of the mixture showed two resonances at δ −11.1 and −11.9.

Stability Tests. ^1H NMR spectra of **1**, **3**, **4**, and $(C_8H_{12})Ir(acac)$ were recorded from CD_3NO_2 solutions 3.5 mM in iridium. Further spectra were then recorded after successive additions of 50 equiv (based on [Ir]) of CD_3CN, up to a total of 250 equiv of CD_3CN, with a ca. 2-min interval between additions. In the case of $(C_8H_{12})Ir(acac)$, the spectrum of the original solution displayed resonances at δ 5.7 (acac CH), 3.8 (C_8H_{12} CH), 2.3 (C_8H_{12} CH_2), 2.0 (acac CH_3), and 1.7 (C_8H_{12} CH_2), and the chemical shifts and relative intensities of these resonances were not significantly changed upon addition of CD_3CN. In the case of compound **4**, the chemical shifts and intensities of the C_8H_{12} ligand resonances (see above) were similarly unaffected by addition of CD_3CN. In the case of compounds **3** and **1**, addition of CD_3CN did affect the ^1H NMR spectra. The chemical shifts of resonances measured from pure CD_3NO_2 solutions are given above. Addition of CD_3CN to **3** in CD_3NO_2 caused a perceptible loss of intensity in the 3.9 ppm resonance after addition of 100 equiv of CD_3CN. After 250 equiv had been added, the δ 3.9 resonance had lost about 20% of its intensity and a small resonance had appeared at δ 4.0. Addition of 50 equiv of CD_3CN/mol of Ir to the CD_3NO_2 solution of **1** caused all the C_8H_{12} resonances for **1** to disappear.

X-ray Crystallographic Study[11] of $\{[(C_8H_{12})Ir]_2H(Nb_2W_4O_{19})_2\}[(n\text{-}C_4H_9)_4N]_5$ (3). Single crystals of $\{[(C_8H_{12})Ir]_2H(Nb_2W_4O_{19})_2\}[(n\text{-}C_4H_9)_4N]_5$ (3) were obtained from 1,2-dichloroethane/toluene in the presence of acetic acid as described above. Details of the crystal structure determination are summarized in Table I.

Table I. Crystallographic Data for $\{[(C_8H_{12})Ir]_2H(Nb_2W_4O_{19})_2\}[(n\text{-}C_4H_9)_4N]_5$ (3) and $[(C_8H_{12})Ir(P_3O_9)][(n\text{-}C_4H_9)_4N]_2$ (4)

	3	4
formula	$C_{96}H_{205}N_5Ir_2Nb_4W_8O_{38}$	$C_{40}H_{84}N_2IrP_3O_9$
fw	4264.6	1022.3
space group	$P\bar{1}$-C_i^1 (No. 2)[12a]	$P2_1/c$-C_{2h}^5 (No. 14)[12b]
cell constants		
a, Å	16.618 (4)	11.324 (2)
b, Å	16.548 (4)	13.288 (2)
c, Å	30.729 (6)	34.035 (5)
α, deg	87.02 (2)	90.00
β, deg	94.57 (2)	101.24 (1)
γ, deg	114.20 (2)	90.00
v, $Å^3$	7681 (3)	5023 (1)
Z	2	4
ρ_{calcd}, g cm^{-3}	1.844	1.352
temp, °C	20 (1)	20 (1)
μ, cm^{-1}	81	63
transm coeff	0.32–1.00	0.06–0.49
radiation	Mo ($K\bar{\alpha}$)[13a]	Cu ($K\bar{\alpha}$)[13a]
$R(F_o)$	0.068	0.065
$R_w(F_o)$	0.078	0.083

A total of 10 506 independent reflections having 2θ(Mo $K\bar{\alpha}$) < 35.9° (the equivalent of 0.30 limiting Cu $K\bar{\alpha}$ spheres) were collected on a computer-controlled four-circle Nicolet autodiffractometer in concentric shells of increasing 2θ using 1.0°-wide ω scans and graphite-monochromated Mo $K\bar{\alpha}$ radiation for a rectangular parallelepiped shaped specimen with dimensions of 0.24 × 0.43 × 0.58 mm. The crystal was sealed with mother liquor in a thin-walled glass capillary and mounted on the diffractometer with its longest edge nearly parallel to the ϕ axis. A scanning rate of 6°/min was used for those reflections having 3.0° < 2θ < 31.3° and a rate of 3°/min was used for all others. The data collection and reduction procedures that were used are described elsewhere.[8] In the present study, counts were accumulated for 17 equal time intervals during the scan, and those 13 contiguous intervals that had the highest single accumulated count at their midpoint were used to calculate the net intensity; the scan width and step-off for background measurements were both 1.00°, and the ratio of total background counting time to net scanning time was 0.50. The intensity data were corrected empirically for variable absorption effects by using ϕ scans for five reflections having 2θ between 4.5 and 25.5°; the relative transmission factors ranged from 0.32 to 1.00. The 14 metal atoms of the asymmetric unit were located by using (SHELXTL) "direct methods" techniques, and counterweighted anisotropic full-matrix least-squares refinement of the structural parameters for these 14 metals gave R_1 (unweighted, based on F)[14] = 0.177 for 4932 independent absorption-corrected reflections having 2θ (Mo $K\bar{\alpha}$) < 35.9° and $I > 3\sigma(I)$. A series of difference Fourier syntheses based on increasingly more complete structural models revealed the remainder of the non-hydrogen atoms for the anions and most of those for the cations of **3**. However, the very low average intensity and limited resolution (maximum $(\sin\theta)/\lambda = 0.43$) of the diffraction data, which was presumably due to disorder of some of the $(n\text{-}C_4H_9)_4N^+$ cations, prevented the location of all non-hydrogen atoms in the cations. Only 129 of the remaining 139 non-hydrogen atoms for **3** could be located and refined: methylene or terminal methyl carbon atoms C_{d2} of cation 2, C_{d2} and C_{d4} of cation 3, C_{b4}, C_{g4}, and C_{d4} of cation 4, and C_{b1}, C_{g1}, C_{d1}, and C_{d2} of cation 5 could not be located. Of the locatable non-hydrogen atoms in the cations of **3**, only those in cations 1–3 could be refined as individual unconstrained isotropic atoms. The locatable non-hydrogen atoms of cations 4 and 5 refined reasonably only when all N–C and C–C bond distances were constrained to a common least-squares-refined value of 1.63 Å and all first and third atoms in a continuous chain were constrained to be 2.67 Å apart.

A structural model that utilized anisotropic thermal parameters for the 14 metal atoms and isotropic thermal parameters for the other 129 locatable non-hydrogen atoms of **3** has been refined to convergence (R_1 = 0.068 and R_2 = 0.078 for 4932 independent absorption-corrected reflections) by using counter-weighted[15] cascade block-diagonal least-squares techniques.

X-ray Crystallographic Study[11] of $[(C_8H_{12})Ir(P_3O_9)][(n\text{-}C_4H_9)_4N]_2$ (4). Single crystals of $[(C_8H_{12})Ir(P_3O_9)][(n\text{-}C_4H_9)_4N]_2$ (4) were obtained as described above. Details of the crystal structure determination are summarized in Table I.

A total of 4625 independent reflections having 2θ(Cu $K\bar{\alpha}$) < 94.9° (the equivalent of 0.40 limiting Cu $\bar{K}\alpha$ spheres) were collected on a computer-controlled four-circle Nicolet autodiffractometer using 2.0°-wide θ–2θ scans and Ni-filtered Cu $K\bar{\alpha}$ radiation for a flat, parallelepiped-shaped specimen with dimensions of 0.113 × 0.500 × 0.575 mm. The crystal was sealed with mother liquor in a thin-walled glass capillary and mounted on the diffractometer with its longest edge nearly parallel to the ϕ axis. Scanning rates of 6°/min, 3°/min, and 2°/min were used for those reflections having 3.0° < 2θ < 71.6°, 71.6° < 2θ < 84.0°, and 84.0° < 2θ < 94.9°, respectively. The ratio of total background counting time to scanning time was 1.00. The intensity data were corrected for absorption effects with a numerical (Gaussian grid) absorption correction;

---

(11) See paragraph at end of paper regarding supplementary material.

(12) *International Tables for X-ray Crystallography*; Kynoch: Birmingham, England, 1969; Vol. I: (a) p 75; (b) p 99.

(13) *International Tables for X-ray Crystallography*; Kynoch: Birmingham, England, 1974; Vol. IV: (a) pp 55–66; (b) pp 99–101; (c) pp 149–150.

(14) The R values are defined as $R_1 = \sum||F_o| - |F_c||/\sum|F_o|$ and $R_2 = \{\sum w(|F_o| - |F_c|)^2/\sum w|F_o|^2\}^{1/2}$, where $w = [\sigma(F)]^{-2}$ is the weight given each reflection. The function minimized is $\sum w(|F_o| - K|F_c|)^2$, where K is the scale factor.

(15) For counter weights: $\sigma(F) = \{[\sigma(F_o)]^2 + (p|F_o|)^2\}^{1/2}$, where the "ignorance factor", p, has the value 0.03 in this case.

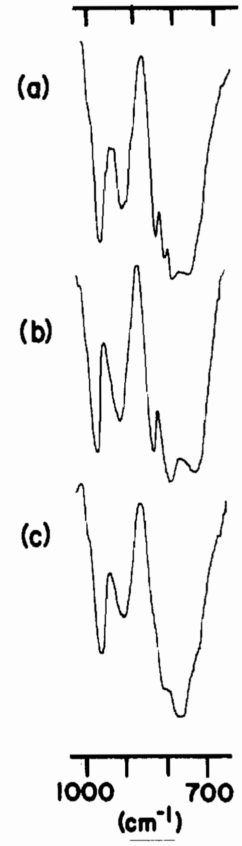

Figure 1. IR spectra of (a) $\{[(C_7H_8)Rh]_5(Nb_2W_4O_{19})_2\}[(n\text{-}C_4H_9)_4N]_3$, (b) $\{[(C_8H_{12})Ir]_5(Nb_2W_4O_{19})_2\}[(n\text{-}C_4H_9)_4N]_3$, and (c) $\{[(C_8H_{12})Ir]_2H(Nb_2W_4O_{19})_2\}[(n\text{-}C_4H_9)_4N]_5$ measured from Nujol mulls between KBr plates. See Experimental Section for numerical data.

the transmission factors ranged from 0.056 to 0.487. The structure was solved by using the "heavy-atom" technique.

A structural model that utilized anisotropic thermal parameters for the non-hydrogen atoms of the anion and isotropic thermal parameters for all locatable non-hydrogen atoms of the cations has been refined to convergence [R_1 (unweighted, based on F)[14] = 0.065 and R_2 (weighted, based on F)[14] = 0.083 for 1499 independent absorption-corrected reflections having $2\theta(\text{Cu } K\bar{\alpha}) < 94.9°$ and $I > 3\sigma(I)$] by using counter-weighted[15] cascade block-diagonal least-squares techniques. The second cation appears to be disordered in the solid state; methylene carbon atom C_{g2} of this cation appears to be statistically disordered in the lattice between two possible sites, C_{g2} and C_{g2}', and terminal methyl carbon atom C_{d2} could not be located from difference Fourier syntheses.

All structure factor calculations for **3** and **4** employed recent tabulations of atomic form factors[13b] and anomalous dispersion corrections[13c] to the scattering factors of any W, Nb, Ir, or P atoms that were present. The final cycles of refinement for both compounds utilized a least-squares-refineable extinction correction.[16] All calculations were performed on a Data General Eclipse S-200 or S-230 computer equipped with 512K of 16-bit words, a floating point processor for 32- and 64-bit arithmetic, and versions of the Nicolet EXTL and SHELXTL interactive crystallographic software package as modified at Crystalytics Co.

Results and Discussion

$\{[(C_8H_{12})Ir]_5(Nb_2W_4O_{19})_2\}[(n\text{-}C_4H_9)_4N]_3$ (1). Reaction of $[(C_8H_{12})Ir(NCCH_3)_2]PF_6$ with $Nb_2W_4O_{19}[(n\text{-}C_4H_9)_4N]_4$ in CH_2Cl_2 solution according to eq 1 results in the formation of

$$5(C_8H_{12})Ir(NCCH_3)_2^+ + 2Nb_2W_4O_{19}^{4-} \rightarrow [(C_8H_{12})Ir]_5(Nb_2W_4O_{19})_2^{3-} + 10CH_3CN \quad (1)$$

$\{[(C_8H_{12})Ir]_5(Nb_2W_4O_{19})_2\}[(n\text{-}C_4H_9)_4N]_3$ (**1**). The product crystallizes directly from the reaction solution as orange microcrystals in >80% yield and is formulated as a 5:2 adduct on the basis of elemental analysis. Compound **1** displays five resonances of equal intensity in the coordinated olefin region of its $^{13}C\{^1H\}$ NMR spectrum (see Experimental Section). Its IR spectrum is very similar to the spectrum of the (norbornadiene)rhodium(I) complex $\{[(C_7H_8)Rh]_5(Nb_2W_4O_{19})_2\}[(n\text{-}C_4H_9)_4N]_3$ (**2**)[2a] in the 700–1000-cm^{-1} region (see Figure 1). The anion of **1** is therefore assumed to have the C_{2v} structure adopted by the anion of **2**, where two octahedral $Nb_2W_4O_{19}^{4-}$ anions are linked together in a face-to-face fashion by five organometallic centers as shown in a and b of Chart I: three of the five iridium atoms are bonded to doubly bridging ONbW or ONb_2 oxygens, and the other two are bonded to terminal ONb oxygens.[2a]

Chart I

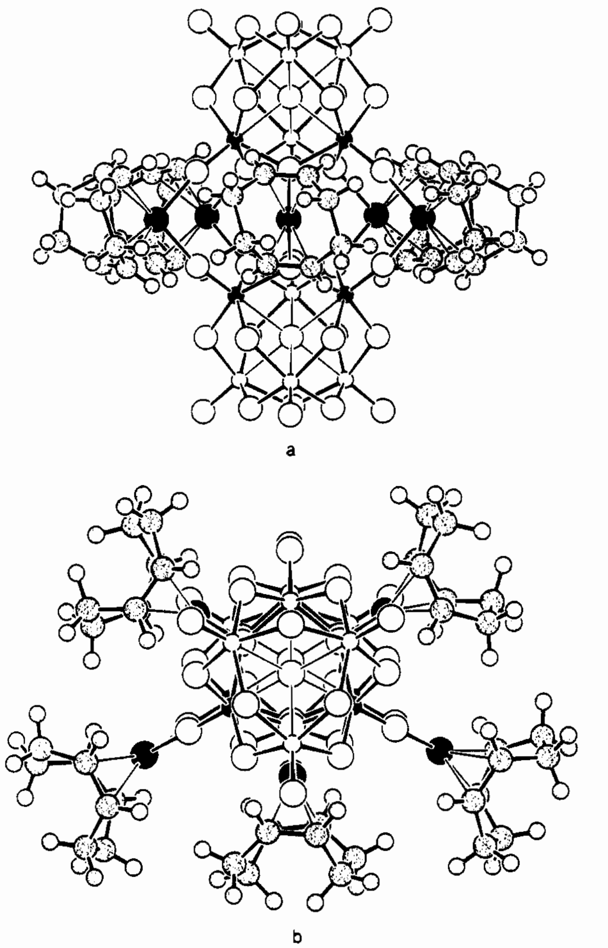

$\{[(C_8H_{12})Ir]_2H(Nb_2W_4O_{19})_2\}[(n\text{-}C_4H_9)_4N]_5$ (3). Reaction of compound **1** with $Nb_2W_4O_{19}[(n\text{-}C_4H_9)_4N]_4$ and CH_3COOH in CH_3CN solution according to eq 2 followed by recrystallization

$$2\{[(C_8H_{12})Ir]_5(Nb_2W_4O_{19})_2\}^{3-} + 6Nb_2W_4O_{19}^{4-} + 5H^+ \rightarrow 5\{[(C_8H_{12})Ir]_2H(Nb_2W_4O_{19})_2\}^{5-} \quad (2)$$

of the crude product yields a crystalline material in ≃50% yield containing $(C_8H_{12})Ir^+$, $Nb_2W_4O_{19}^{4-}$, and $(n\text{-}C_4H_9)_4N^+$ in a ratio of 2:2:5 according to elemental analysis. With addition of a proton to obtain charge balance, the empirical formula $\{[(C_8H_{12})Ir]_2H(Nb_2W_4O_{19})_2\}[(n\text{-}C_4H_9)_4N]_5$ (**3**) is obtained, a formulation supported by elemental analysis, X-ray crystallography, and ^{17}O NMR spectroscopy.

X-ray structural analysis revealed that single crystals of $\{[(C_8H_{12})Ir]_2H(Nb_2W_4O_{19})_2\}[(n\text{-}C_4H_9)_4N]_5$ (**3**) are composed of discrete $(n\text{-}C_4H_9)_4N^+$ cations (Figure S1[11]) and $\{[(C_8H_{12})Ir]_2H(Nb_2W_4O_{19})_2\}^{5-}$ anions (Figures 2 and 3) in which two cis-$Nb_2W_4O_{19}^{4-}$ anions are bridged by a single proton and two (cyclooctadiene)iridium(I) cations. Final atomic coordinates and thermal parameters for non-hydrogen atoms of **3** are given with estimated standard deviations in Tables II and S1,[11] respectively. Bond lengths and angles for the $\{[(C_8H_{12})Ir]_2H(Nb_2W_4O_{19})_2\}^{5-}$ anions are given in Table III, and bond lengths and angles for the $(n\text{-}C_4H_9)_4N^+$ cations of **3** are given in Table S2.[11]

---

[16] Larson, A. C. *Acta Crystallogr.* **1967**, *23*, 664.

Scheme I

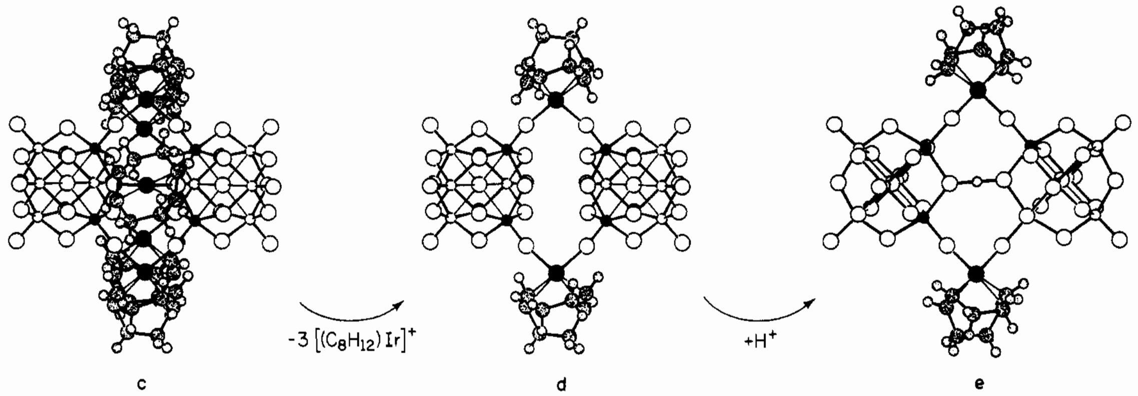

Both crystallographically independent $\{[(C_8H_{12})Ir]_2H(Nb_2W_4O_{19})_2\}^{5-}$ anions in **3** appear to possess rigorous C_i symmetry in the solid state: their non-hydrogen atoms are symmetrically disposed about the crystallographic inversion centers at (0, 0, 0) and ($^1/_2$, $^1/_2$, $^1/_2$) of the unit cell. The two Ir(I) centers in each dimeric anion are both square-planar d^8 16-electron metal centers with one pair of cis coordination sites occupied by the olefinic C=C bonds of a single cyclooctadiene ligand and the other pair by terminal ONb oxygens from two different cis-$Nb_2W_4O_{19}^{4-}$ anions. Scheme I shows the relationship between the anion structure of **3** (see e) and the structure proposed for the $\{[(C_8H_{12})Ir]_5(Nb_2W_4O_{19})_2\}^{3-}$ anion in compound **1** (see c). Removal of all three $(C_8H_{12})Ir^+$ units in c that are bonded to ONbW and ONb_2 oxygens of the $Nb_2W_4O_{19}^{4-}$ ligands without relaxing the geometry of the resulting species gives the hypothetical C_{2v}-$[(C_8H_{12})Ir]_2(Nb_2W_4O_{19})_2^{6-}$ anion d, in which only the $(C_8H_{12})Ir^+$ units bonded to terminal ONb oxygens remain. Addition of a proton between the two ONb_2 oxygens (see below) plus conformational relaxation to an approximately D_{2h} configurations produces the structure shown in e.

The two $\{[(C_8H_{12})Ir]_2H(Nb_2W_4O_{19})_2\}^{5-}$ anions have similar conformations in the solid state that deviate significantly from idealized D_{2h} symmetry. The four O_G atoms of each dimer are required by crystallographic C_i symmetry to be coplanar[17a,b] and describe rectangles with edge lengths of 6.083 (3, 12, 12, 2)[19] and 2.71 Å (3, 1, 1, 2); the cis-$Nb_2W_4O_{19}^{4-}$ anions span the longer edges, and the $(C_8H_{12})Ir^+$ cations are attached across the shorter edges. The $(C_8H_{12})Ir(O_G)_2$ "squares"[17c,d] and the Nb_2W_2 "squares"[17e,f] of the $Nb_2W_4O_{19}^{4-}$ anions for each dimer make average dihedral angles of 20.1 (-, 26, 26, 2)[19] and 13.4° (-, 38, 38, 2), respectively, with the $4O_G$ rectangle. These pairs of squares thus form "steps" with the following average[19] distances between opposite pairs of C_i-related planar atomic groupings: 2.03 Å (-, 30, 30, 2) between nearly coplanar (to within 0.09 Å)[17c,d] O_{G1}, O_{G2}', Ir, $C_{1,2}$,[18] and $C_{5,6}$[18] groupings and 0.57 Å (-, 15, 15, 2) between nearly coplanar (to within 0.08 Å) Nb_1, Nb_2, W_3, W_4, O_A, O_B, O_{D3}, O_{D4}, O_F, O_{G1}, O_{G2}, O_{H3}, and O_{H4} groupings.

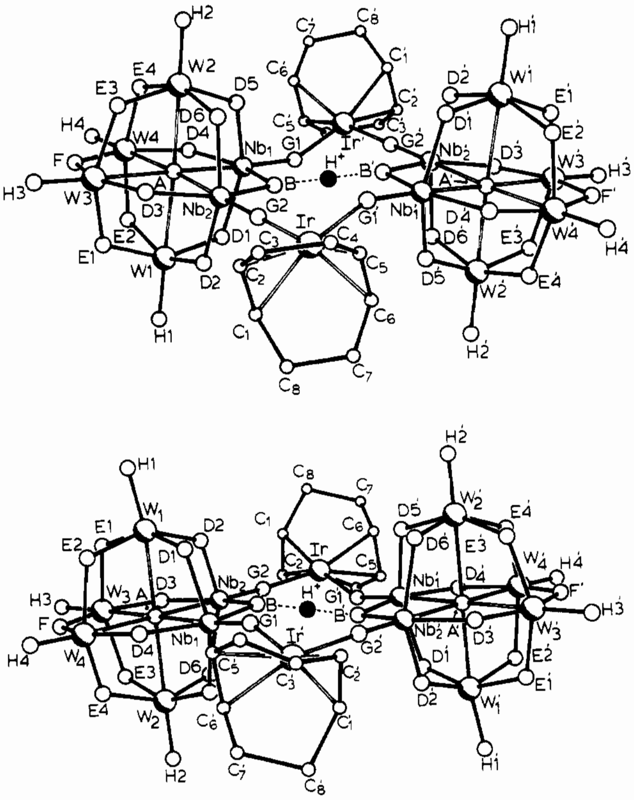

Figure 2. Perspective drawings of the two crystallographically independent $\{[(C_8H_{12})Ir]_2H(Nb_2W_4O_{19})_2\}^{5-}$ anions in crystalline $\{[(C_8H_{12})Ir]_2H(Nb_2W_4O_{19})_2\}[(n\text{-}C_4H_9)_4N]_5$: (a, top) anion I; (b, bottom) anion II. Both views are nearly parallel to the planar Ir coordination groups and the Ir → Ir vector. Ir, Nb, and W atoms are represented by large shaded spheres; oxygen and carbon atoms are represented by medium-sized and small open spheres, respectively. Hydrogen atoms on the COD ligands are not shown. Atoms labeled with a prime (′) are related to those without by the crystallographic inversion center at (0, 0, 0) in the unit cell for anion I and ($^1/_2$, $^1/_2$, $^1/_2$) in the unit cell for anion II. The single protons associated with each of these dimers are believed to occupy these inversion centers and are represented by blackened spheres.

The hydrogen atoms of **3** could not be located directly from difference Fourier syntheses, but approximate positions for the single proton of each $\{[(C_8H_{12})Ir]_2H(Nb_2W_4O_{19})\}^{5-}$ dimer can be reasonably inferred from the metrical parameters of the non-hydrogen atoms. Even though both independent Ir atoms are clearly square-planar d^8 species, the O···O contacts and O–Ir–O bond angles of both coordination groups and the intraionic steps between them noted above are somewhat unusual and suggestive of a strong hydrogen bond between the two cis-$Nb_2W_4O_{19}^{4-}$ polyoxoanions of each $\{[(C_8H_{12})Ir]_2H(Nb_2W_4O_{19})_2\}^{5-}$ dimer. The independent O_{G1}'···O_{G2} separations of 2.71 and 2.72 Å are ≥0.08

---

(17) The least-squares mean planes for the following groups of atoms in **3** are defined by the equation $ax + by + cz = d$, where x, y, and z are orthogonal coordinates measured along $\vec{a}$, $\vec{b}^*$, and $\vec{a} \times \vec{b}^*$, respectively, of the crystal system. (a) O_{G1}, O_{G2}, O_{G1}', and O_{G2}' for anion I (required by symmetry to be totally coplanar): $a = -0.375$, $b = 0.890$, $c = 0.260$, $d = 0.000$. (b) O_{G1}, O_{G2}, O_{G1}', and O_{G2}' for anion II (required by symmetry to be totally coplanar): $a = -0.216$, $b = 0.827$, $c = 0.520$, $d = 10.279$. (c) $C_{1,2}$,[18] $C_{5,6}$,[18] O_{G1}', and O_{G2} for anion I (coplanar to within 0.06 Å): $a = -0.698$, $b = 0.665$, $c = 0.265$, $d = 1.159$. (d) $C_{1,2}$,[18] $C_{5,6}$,[18] Ir, O_{G1}', and O_{G2} for anion II (coplanar to within 0.10 Å): $a = -0.497$, $b = 0.715$, $c = 0.492$, $d = 6.312$. (e) Nb_1, Nb_2, W_3, and W_4 for anion I (coplanar to within 0.001 Å): $a = 0.317$, $b = -0.785$, $c = -0.533$, $d = 0.428$. (f) Nb_1, Nb_2, W_3, and W_4 for anion II (coplanar to within 0.005 Å): $a = -0.309$, $b = 0.868$, $c = 0.388$, $d = 7.640$.

(18) $C_{1,2}$ and $C_{5,6}$ refer to the midpoints of the C_1–C_2 and C_5–C_6 olefinic bonds, respectively.

(19) The first number in parentheses following an average value of a bond length or angle is the root-mean-square estimated standard deviation of an individual datum. The second and third numbers are the average and maximum deviations from the average value, respectively. The fourth number represents the number of individual measurements that are included in the average value.

Table II. Fractional Atomic Coordinates for Non-Hydrogen Atoms in Crystalline $\{[(C_8H_{12})Ir]_2H(Nb_2W_4O_{19})_2\}[(n\text{-}C_4H_9)_4N]_5$ (**3**)[a]

atom type[b]	10^3x	10^3y	10^3z	B,[c] Å^2	atom type[b]	10^3x	10^3y	10^3z	B,[c] Å^2
Anion I									
W_1	−1.9 (1)	−11.1 (1)	−160.1 (1)	5.5 (1)	O_{E3}	−183 (2)	123 (2)	−135 (1)	7 (1)
W_2	−97.7 (1)	171.5 (1)	−89.8 (1)	5.6 (1)	O_{E4}	−34 (2)	242 (2)	−133 (1)	6 (1)
W_3	−174.4 (1)	40.3 (1)	−174.4 (1)	5.6 (1)	O_F	−82 (2)	141 (2)	−202 (1)	6 (1)
W_4	27.4 (1)	199.9 (1)	−172.1 (1)	5.6 (1)	O_{G1}	172 (2)	160 (2)	−40 (1)	7 (1)
Nb_1	75.7 (3)	123.3 (3)	−77.4 (2)	4.9 (2)	O_{G2}	−191 (2)	−129 (2)	−47 (1)	8 (1)
Nb_2	−129.6 (3)	−38.9 (3)	−79.7 (2)	5.1 (2)	O_{H1}	36 (3)	−76 (2)	−186 (2)	12 (1)
Ir	−253.8 (1)	−235.4 (1)	−6.4 (1)	5.2 (1)	O_{H2}	−131 (2)	240 (2)	−66 (1)	10 (1)
O_A	−50 (1)	81 (1)	−123 (1)	3 (1)	O_{H3}	−263 (2)	14 (2)	−210 (1)	6 (1)
O_B	−17 (2)	15 (2)	−45 (1)	6 (1)	O_{H4}	85 (2)	281 (2)	−208 (1)	7 (1)
O_{D1}	91 (1)	40 (1)	−117 (1)	4 (1)	C_1	−294 (3)	−320 (3)	−59 (2)	5 (1)
O_{D2}	−75 (1)	−89 (1)	−117 (1)	4 (1)	C_2	−358 (3)	−285 (3)	−52 (2)	6 (1)
O_{D3}	−223 (2)	−45 (2)	−127 (1)	6 (1)	C_3	−453 (3)	−336 (3)	−24 (2)	8 (1)
O_{D4}	112 (2)	211 (1)	−126 (1)	4 (1)	C_4	−442 (3)	−356 (3)	28 (2)	8 (1)
O_{D5}	17 (2)	185 (2)	−59 (1)	5 (1)	C_5	−332 (3)	−320 (3)	36 (2)	7 (1)
O_{D6}	−152 (2)	61 (2)	−59 (1)	5 (1)	C_6	−266 (3)	−349 (3)	27 (2)	5 (1)
O_{E1}	−117 (2)	−24 (2)	−192 (1)	7 (1)	C_7	−311 (4)	−434 (4)	6 (3)	12 (2)
O_{E2}	53 (2)	107 (2)	−192 (1)	7 (1)	C_8	−322 (3)	−419 (3)	−44 (2)	8 (1)
Anion II									
W_1	362.8 (2)	644.9 (2)	399.7 (1)	7.4 (1)	O_{E3}	488 (2)	528 (2)	313 (1)	11 (1)
W_2	456.2 (2)	438.4 (2)	352.6 (1)	8.6 (1)	O_{E4}	330 (2)	410 (2)	325 (1)	9 (1)
W_3	463.5 (2)	632.7 (2)	314.5 (1)	7.9 (1)	O_F	350 (2)	558 (2)	297 (1)	9 (1)
W_4	273.4 (1)	471.1 (1)	336.3 (1)	6.2 (1)	O_{G1}	292 (2)	379 (2)	483 (1)	8 (1)
Nb_1	352.2 (3)	450.5 (3)	435.6 (2)	7.5 (2)	O_{G2}	655 (2)	673 (2)	439 (1)	9 (1)
Nb_2	547.9 (3)	615.2 (3)	413.4 (2)	6.1 (2)	O_{H1}	322 (3)	721 (2)	409 (2)	12 (1)
Ir	757.0 (1)	728.8 (1)	482.9 (1)	7.4 (1)	O_{H2}	483 (2)	363 (2)	338 (1)	11 (1)
O_A	411 (2)	543 (1)	376 (1)	4 (1)	O_{H3}	492 (3)	694 (3)	268 (2)	18 (2)
O_B	473 (2)	527 (2)	461 (1)	6 (1)	O_{H4}	178 (2)	426 (2)	309 (1)	10 (1)
O_{D1}	328 (2)	558 (2)	438 (1)	7 (1)	C_1	795 (3)	848 (3)	452 (2)	7 (1)
O_{D2}	489 (2)	680 (2)	424 (1)	8 (1)	C_2	835 (4)	807 (4)	432 (2)	11 (2)
O_{D3}	560 (2)	671 (2)	355 (1)	7 (1)	C_3	925 (5)	848 (4)	453 (3)	11 (2)
O_{D4}	250 (2)	414 (2)	392 (1)	6 (1)	C_4	946 (6)	798 (5)	486 (3)	17 (3)
O_{D5}	400 (2)	381 (2)	409 (1)	6 (1)	C_5	882 (5)	754 (4)	523 (3)	12 (2)
O_{D6}	557 (2)	513 (2)	381 (1)	7 (1)	C_6	837 (3)	803 (3)	536 (2)	8 (1)
O_{E1}	410 (2)	693 (2)	344 (1)	5 (1)	C_7	877 (5)	894 (5)	528 (3)	18 (3)
O_{E2}	257 (2)	568 (2)	363 (1)	7 (1)	C_8	834 (5)	933 (5)	484 (3)	15 (2)
Cation 1									
N	−206 (3)	140 (3)	62 (2)	10 (1)	C_{g1}	−236 (5)	111 (5)	183 (3)	13 (2)
C_{a1}	−209 (3)	100 (3)	110 (2)	8 (1)	C_{g2}	37 (5)	229 (5)	46 (3)	14 (2)
C_{a2}	−101 (5)	220 (4)	56 (2)	12 (2)	C_{g3}	−309 (6)	291 (5)	20 (3)	20 (3)
C_{a3}	−255 (4)	206 (3)	61 (2)	10 (2)	C_{g4}	−346 (7)	−79 (7)	16 (4)	21 (4)
C_{a4}	−232 (5)	52 (5)	38 (3)	13 (2)	C_{d1}	−197 (6)	163 (6)	216 (4)	20 (4)
C_{b1}	−195 (5)	170 (5)	142 (3)	16 (3)	C_{d2}	59 (6)	316 (6)	46 (4)	22 (4)
C_{b2}	−65 (5)	168 (5)	61 (3)	13 (2)	C_{d3}	−340 (9)	328 (8)	−39 (5)	38 (7)
C_{b3}	−273 (4)	213 (4)	8 (2)	11 (2)	C_{d4}	−406 (7)	−92 (7)	−13 (4)	26 (5)
C_{b4}	−339 (8)	6 (7)	40 (4)	25 (5)					
Cation 2[d]									
N	328 (3)	272 (3)	210 (2)	8 (1)	C_{b4}	442 (6)	228 (5)	200 (3)	16 (3)
C_{a1}	335 (3)	249 (3)	261 (2)	8 (1)	C_{g1}	306 (6)	127 (6)	321 (4)	20 (4)
C_{a2}	374 (4)	371 (4)	218 (2)	10 (2)	C_{g2}	424 (7)	536 (7)	181 (4)	23 (4)
C_{a3}	236 (3)	264 (3)	195 (2)	7 (1)	C_{g3}	104 (7)	286 (7)	211 (4)	20 (4)
C_{a4}	357 (6)	212 (5)	187 (3)	17 (3)	C_{g4}	483 (7)	211 (6)	146 (4)	19 (4)
C_{b1}	286 (5)	148 (4)	272 (2)	15 (2)	C_{d1}	255 (10)	160 (10)	354 (3)	49 (10)
C_{b2}	395 (5)	412 (4)	174 (3)	14 (2)	C_{d3}	74 (5)	336 (5)	204 (3)	17 (3)
C_{b3}	190 (7)	291 (6)	232 (4)	19 (4)	C_{d4}	553 (6)	198 (5)	164 (3)	19 (3)
Cation 3[d]									
N	−188 (4)	296 (3)	742 (2)	14 (2)	C_{b4}	−161 (8)	232 (7)	673 (5)	23 (4)
C_{a1}	−279 (6)	300 (5)	733 (3)	19 (3)	C_{g1}	−408 (9)	149 (9)	717 (5)	33 (6)
C_{a2}	−138 (4)	391 (4)	714 (3)	12 (2)	C_{g2}	32 (6)	548 (6)	702 (4)	22 (4)
C_{a3}	−127 (7)	340 (6)	786 (4)	22 (4)	C_{g3}	−142 (6)	395 (5)	852 (3)	16 (3)
C_{a4}	−149 (6)	247 (5)	728 (4)	17 (3)	C_{g4}	−95 (8)	193 (7)	660 (4)	26 (5)
C_{b1}	−312 (6)	202 (5)	763 (3)	19 (3)	C_{d1}	−481 (5)	55 (5)	746 (3)	18 (3)
C_{b2}	−38 (6)	443 (6)	733 (3)	18 (3)	C_{d3}	−203 (7)	434 (6)	879 (4)	22 (4)
C_{b3}	−223 (8)	341 (7)	818 (4)	23 (4)					
Cation 4[d]									
N	669 (1)	317 (1)	437 (1)	22 (3)	C_{b3}	602 (2)	282 (5)	355 (1)	31 (6)
C_{a1}	570 (1)	250 (1)	449 (1)	25 (4)	C_{g1}	421 (2)	233 (2)	482 (3)	22 (4)
C_{a2}	679 (1)	420 (1)	437 (1)	16 (3)	C_{g2}	781 (4)	584 (3)	410 (5)	36 (7)
C_{a3}	688 (1)	295 (2)	388 (1)	23 (4)	C_{g3}	603 (2)	225 (5)	313 (1)	29 (5)
C_{a4}	742 (1)	305 (1)	472 (1)	19 (4)	C_{d1}	415 (4)	132 (1)	481 (4)	28 (5)
C_{b1}	521 (2)	303 (1)	471 (2)	27 (5)	C_{d2}	870 (8)	641 (5)	385 (5)	42 (8)
C_{b2}	778 (2)	486 (1)	423 (3)	23 (4)	C_{d3}	705 (4)	251 (6)	302 (3)	33 (6)

Table II (Continued)

atom type[b]	10^3x	10^3y	10^3z	*B*,[c] Å^2	atom type[b]	10^3x	10^3y	10^3z	*B*,[c] Å^2
				Cation 5[d]					
N	230 (1)	153 (1)	722 (1)	40 (6)	C_{b4}	322 (6)	81 (5)	682 (2)	25 (4)
C_{a1}	141 (1)	63 (1)	727 (1)	19 (4)	C_{g2}	323 (5)	170 (5)	849 (1)	23 (4)
C_{a2}	300 (1)	159 (1)	763 (1)	16 (3)	C_{g3}	270 (2)	414 (4)	728 (1)	37 (7)
C_{a3}	206 (1)	239 (1)	720 (1)	40 (7)	C_{g4}	383 (4)	93 (4)	642 (2)	17 (3)
C_{a4}	274 (1)	150 (1)	676 (1)	21 (4)	C_{d3}	275 (8)	471 (5)	683 (2)	28 (5)
C_{b2}	272 (4)	192 (5)	806 (1)	31 (6)	C_{d4}	330 (9)	14 (8)	607 (3)	41 (8)
C_{b3}	295 (1)	330 (4)	720 (2)	25 (4)					

[a] The numbers in parentheses are the estimated standard deviations in the last significant digit. [b] Atoms are labeled in agreement with Figures 2, 3, and S1.[11] [c] Isotropic thermal parameter; for metal atoms, this is one-third of the trace of the orthogonalized $\mathbf{B}_{ij}$ tensor. [d] Carbon atoms C_{d2} of cation 2, C_{d2} and C_{d4} of cation 3, C_{b4}, c_{g4}, and C_{d4} of Cation 4, and C_{b1}, C_{g1}, C_{d1}, and C_{d2} of cation 5 could not be located or refined.

Table III. Bond Lengths (Å) and Angles (deg) in the $\{[(C_8H_{12})Ir]_2H(Nb_2W_4O_{19})_2\}^{5-}$ Anions of Crystalline $\{[(C_8H_{12})Ir]_2H(Nb_2W_4O_{19})_2\}[(n\text{-}C_4H_9)_4N]_5$ (3)[a]

	values			values			values			values	
type[b]	anion I	anion II	type[b]	anion I	anion II	type[b]	anion I	anion II	type[b]	anion I	anion II
						Bond Lengths					
$\mathrm{Ir{-}C_{1}}$	2.07 (5)	2.02 (5)	$\mathrm{W_{2}{-}O_{A}}$	2.28 (3)	2.32 (3)	$\mathrm{W_{1}{-}O_{D1}}$	1.89 (2)	1.74 (3)	$\mathrm{W_{1}{-}O_{H1}}$	1.72 (5)	1.70 (5)
$\mathrm{Ir{-}C_{2}}$	2.04 (5)	2.12 (7)	$\mathrm{W_{3}{-}O_{A}}$	2.38 (2)	2.33 (3)	$\mathrm{W_{1}{-}O_{D2}}$	1.92 (2)	2.02 (3)	$\mathrm{W_{2}{-}O_{H2}}$	1.67 (4)	1.59 (5)
$\mathrm{Ir{-}C_{5}}$	1.98 (5)	2.22 (7)	$\mathrm{W_{4}{-}O_{A}}$	2.39 (2)	2.36 (2)	$\mathrm{W_{2}{-}O_{D5}}$	1.98 (3)	2.02 (3)	$\mathrm{W_{3}{-}O_{H3}}$	1.68 (3)	1.70 (6)
$\mathrm{Ir{-}C_{6}}$	2.04 (4)	2.12 (6)	$\mathrm{Nb_{1}{-}O_{B}}$	2.09 (3)	2.01 (3)	$\mathrm{W_{2}{-}O_{D6}}$	1.91 (2)	1.81 (3)	$\mathrm{W_{4}{-}O_{H4}}$	1.75 (3)	1.63 (4)
$\mathrm{Ir{-}C_{g1,2}}$[c]	1.93	1.97	$\mathrm{Nb_{2}{-}O_{B}}$	1.96 (3)	2.10 (3)	$\mathrm{W_{3}{-}O_{D3}}$	1.95 (3)	1.85 (3)	$\mathrm{C_{1}{-}C_{2}}$	1.42 (8)	1.31 (10)
$\mathrm{Ir{-}C_{g5,6}}$[c]	1.88	2.05	$\mathrm{Nb_{1}{-}O_{D1}}$	1.99 (3)	1.99 (3)	$\mathrm{W_{4}{-}O_{D4}}$	1.87 (3)	1.91 (3)	$\mathrm{C_{1}{-}C_{8}}$	1.56 (7)	1.63 (9)
$\mathrm{Ir{-}O_{G1}'}$[d]	1.99 (3)	1.93 (3)	$\mathrm{Nb_{2}{-}O_{D2}}$	1.93 (3)	1.77 (4)	$\mathrm{W_{1}{-}O_{E1}}$	2.02 (3)	1.92 (3)	$\mathrm{C_{2}{-}C_{3}}$	1.73 (7)	1.48 (9)
$\mathrm{Ir{-}O_{G2}}$	2.04 (3)	2.00 (3)	$\mathrm{Nb_{2}{-}O_{D3}}$	2.01 (3)	1.97 (3)	$\mathrm{W_{1}{-}O_{E2}}$	2.02 (3)	2.00 (3)	$\mathrm{C_{3}{-}C_{4}}$	1.62 (9)	1.38 (13)
$\mathrm{Nb_{1}{-}O_{G1}}$	1.79 (3)	1.89 (3)	$\mathrm{Nb_{1}{-}O_{D4}}$	1.98 (3)	1.98 (3)	$\mathrm{W_{2}{-}O_{E3}}$	1.86 (3)	1.80 (4)	$\mathrm{C_{4}{-}C_{5}}$	1.68 (7)	1.55 (12)
$\mathrm{Nb_{2}{-}O_{G2}}$	1.75 (3)	1.78 (3)	$\mathrm{Nb_{1}{-}O_{D5}}$	1.81 (3)	1.89 (4)	$\mathrm{W_{2}{-}O_{E4}}$	1.83 (3)	2.07 (4)	$\mathrm{C_{5}{-}C_{6}}$	1.41 (8)	1.41 (11)
$\mathrm{Nb_{1}{-}O_{A}}$	2.29 (2)	2.33 (3)	$\mathrm{Nb_{2}{-}O_{D6}}$	1.98 (3)	2.08 (4)	$\mathrm{W_{3}{-}O_{E1}}$	1.81 (4)	1.90 (3)	$\mathrm{C_{6}{-}C_{7}}$	1.47 (8)	1.39 (9)
$\mathrm{Nb_{2}{-}O_{A}}$	2.30 (2)	2.33 (2)	$\mathrm{W_{3}{-}O_{F}}$	1.95 (2)	1.84 (3)	$\mathrm{W_{3}{-}O_{E3}}$	1.93 (4)	1.93 (4)	$\mathrm{C_{7}{-}C_{8}}$	1.55 (10)	1.68 (13)
$\mathrm{W_{1}{-}O_{A}}$	2.36 (3)	2.30 (3)	$\mathrm{W_{4}{-}O_{F}}$	1.87 (3)	1.92 (3)	$\mathrm{W_{4}{-}O_{E2}}$	1.89 (3)	1.95 (4)	$\mathrm{O_{B}{\cdots}H}$	1.42 (4)	1.36 (4)
						$\mathrm{W_{4}{-}O_{E4}}$	1.95 (3)	1.70 (4)			
						Bond Angles					
$\mathrm{O_{G1}'IrO_{G2}}$[d]	84 (1)	87 (1)	$\mathrm{W_{2}O_{E4}W_{4}}$	121 (2)	121 (2)	$\mathrm{O_{H2}W_{2}O_{E4}}$	102 (2)	107 (2)	$\mathrm{O_{D4}Nb_{1}O_{D1}}$	86 (1)	83 (1)
$\mathrm{C_{g1,2}IrC_{g5,6}}$[c]	92	92	$\mathrm{W_{3}O_{F}W_{4}}$	120 (2)	122 (2)	$\mathrm{O_{H3}W_{3}O_{D3}}$	102 (1)	109 (2)	$\mathrm{O_{D4}Nb_{1}O_{D5}}$	87 (1)	91 (1)
$\mathrm{O_{G1}'IrC_{g5,6}}$[c,d]	93	89	$\mathrm{Nb_{1}O_{B}H}$	119 (2)	117 (2)	$\mathrm{O_{H3}W_{3}O_{E1}}$	103 (2)	103 (2)	$\mathrm{O_{B}Nb_{2}O_{D2}}$	90 (1)	86 (1)
$\mathrm{O_{G2}IrC_{g1,2}}$[c]	91	91	$\mathrm{Nb_{2}O_{B}H}$	127 (2)	130 (2)	$\mathrm{O_{H3}W_{3}O_{E3}}$	106 (2)	111 (3)	$\mathrm{O_{B}Nb_{2}O_{D6}}$	84 (1)	92 (1)
$\mathrm{O_{G1}'IrC_{g1,2}}$[c,d]	175	170	$\mathrm{C_{8}C_{1}C_{2}}$	114 (4)	131 (5)	$\mathrm{O_{H3}W_{3}O_{F}}$	104 (1)	99 (2)	$\mathrm{O_{D3}Nb_{2}O_{D2}}$	92 (1)	85 (2)
$\mathrm{O_{G2}IrC_{g5,6}}$[c]	174	177	$\mathrm{C_{1}C_{2}C_{3}}$	128 (4)	101 (6)	$\mathrm{O_{H4}W_{4}O_{D4}}$	103 (1)	103 (2)	$\mathrm{O_{D3}Nb_{2}O_{D6}}$	84 (1)	83 (1)
$\mathrm{IrO_{G1}'Nb_{1}'}$	155 (2)	155 (2)	$\mathrm{C_{2}C_{3}C_{4}}$	118 (4)	116 (6)	$\mathrm{O_{H4}W_{4}O_{E2}}$	101 (1)	100 (2)	$\mathrm{O_{D1}W_{1}O_{D2}}$	91 (1)	90 (1)
$\mathrm{IrO_{G2}Nb_{2}}$	175 (2)	165 (2)	$\mathrm{C_{3}C_{4}C_{5}}$	101 (4)	121 (8)	$\mathrm{O_{H4}W_{4}O_{E4}}$	108 (1)	105 (2)	$\mathrm{O_{D1}W_{1}O_{E2}}$	85 (1)	85 (1)
$\mathrm{Nb_{1}O_{A}Nb_{2}}$	94 (1)	93 (1)	$\mathrm{C_{4}C_{5}C_{6}}$	138 (4)	115 (6)	$\mathrm{O_{H4}W_{4}O_{F}}$	104 (1)	105 (2)	$\mathrm{O_{E1}W_{1}O_{D2}}$	85 (1)	87 (1)
$\mathrm{Nb_{1}O_{A}W_{1}}$	90 (1)	90 (1)	$\mathrm{C_{5}C_{6}C_{7}}$	106 (4)	116 (6)	$\mathrm{O_{A}Nb_{1}O_{B}}$	76 (1)	79 (1)	$\mathrm{O_{E1}W_{1}O_{E2}}$	87 (1)	84 (1)
$\mathrm{Nb_{1}O_{A}W_{2}}$	92 (1)	89 (1)	$\mathrm{C_{6}C_{7}C_{8}}$	110 (5)	116 (6)	$\mathrm{O_{A}Nb_{1}O_{D1}}$	77 (1)	71 (1)	$\mathrm{O_{D5}W_{2}O_{D6}}$	88 (1)	93 (1)
$\mathrm{Nb_{1}O_{A}W_{4}}$	89 (1)	89 (1)	$\mathrm{C_{7}C_{8}C_{1}}$	115 (5)	103 (6)	$\mathrm{O_{A}Nb_{1}O_{D4}}$	77 (1)	78 (1)	$\mathrm{O_{D5}W_{2}O_{E4}}$	87 (1)	87 (1)
$\mathrm{Nb_{2}O_{A}W_{1}}$	89 (1)	91 (1)	$\mathrm{O_{A}Nb_{1}O_{G1}}$	177 (1)	172 (1)	$\mathrm{O_{A}Nb_{1}O_{D5}}$	76 (1)	81 (1)	$\mathrm{O_{E3}W_{2}O_{D6}}$	87 (1)	81 (2)
$\mathrm{Nb_{2}O_{A}W_{2}}$	92 (1)	90 (1)	$\mathrm{O_{A}Nb_{2}O_{G2}}$	179 (1)	177 (1)	$\mathrm{O_{A}Nb_{2}O_{B}}$	78 (1)	78 (1)	$\mathrm{O_{E3}W_{2}O_{E4}}$	84 (1)	84 (2)
$\mathrm{Nb_{2}O_{A}W_{3}}$	89 (1)	90 (1)	$\mathrm{O_{A}W_{1}O_{H1}}$	178 (1)	171 (2)	$\mathrm{O_{A}Nb_{2}O_{D2}}$	78 (1)	76 (1)	$\mathrm{O_{D3}W_{3}O_{E1}}$	91 (1)	90 (1)
$\mathrm{W_{1}O_{A}W_{3}}$	88 (1)	90 (1)	$\mathrm{O_{A}W_{2}O_{H2}}$	179 (1)	177 (1)	$\mathrm{O_{A}Nb_{2}O_{D3}}$	80 (1)	75 (1)	$\mathrm{O_{D3}W_{3}O_{E3}}$	84 (1)	84 (2)
$\mathrm{W_{1}O_{A}W_{4}}$	89 (1)	90 (1)	$\mathrm{O_{A}W_{3}O_{H3}}$	179 (1)	175 (2)	$\mathrm{O_{A}Nb_{2}O_{D6}}$	75 (1)	75 (1)	$\mathrm{O_{F}W_{3}O_{E1}}$	85 (1)	85 (1)
$\mathrm{W_{2}O_{A}W_{3}}$	90 (1)	91 (1)	$\mathrm{O_{A}W_{4}O_{H4}}$	179 (1)	178 (2)	$\mathrm{O_{A}W_{1}O_{D1}}$	77 (1)	76 (1)	$\mathrm{O_{F}W_{3}O_{E3}}$	88 (1)	85 (2)
$\mathrm{W_{2}O_{A}W_{4}}$	90 (1)	89 (1)	$\mathrm{O_{G1}Nb_{1}O_{B}}$	104 (1)	106 (1)	$\mathrm{O_{A}W_{1}O_{D2}}$	76 (1)	72 (1)	$\mathrm{O_{D4}W_{4}O_{E2}}$	87 (1)	86 (1)
$\mathrm{W_{3}O_{A}W_{4}}$	88 (1)	89 (1)	$\mathrm{O_{G1}Nb_{1}O_{D1}}$	106 (1)	104 (1)	$\mathrm{O_{A}W_{1}O_{E1}}$	75 (1)	76 (1)	$\mathrm{O_{D4}W_{4}O_{E4}}$	89 (1)	90 (2)
$\mathrm{Nb_{1}O_{A}W_{3}}$	176 (1)	178 (1)	$\mathrm{O_{G1}Nb_{1}O_{D4}}$	103 (1)	97 (1)	$\mathrm{O_{A}W_{1}O_{E2}}$	76 (1)	79 (1)	$\mathrm{O_{F}W_{4}O_{E2}}$	84 (1)	88 (1)
$\mathrm{Nb_{2}O_{A}W_{4}}$	176 (1)	178 (2)	$\mathrm{O_{G1}Nb_{1}O_{D5}}$	101 (1)	105 (1)	$\mathrm{O_{A}W_{2}O_{D5}}$	73 (1)	78 (1)	$\mathrm{O_{F}W_{4}O_{E4}}$	87 (1)	85 (2)
$\mathrm{W_{1}O_{A}W_{2}}$	178 (1)	179 (1)	$\mathrm{O_{G2}Nb_{2}O_{B}}$	103 (1)	105 (1)	$\mathrm{O_{A}W_{2}O_{D6}}$	77 (1)	80 (1)	$\mathrm{O_{B}Nb_{1}O_{D4}}$	153 (1)	157 (1)
$\mathrm{Nb_{1}O_{B}Nb_{2}}$	113 (2)	110 (2)	$\mathrm{O_{G2}Nb_{2}O_{D2}}$	103 (1)	104 (2)	$\mathrm{O_{A}W_{2}O_{E3}}$	76 (1)	73 (2)	$\mathrm{O_{D1}Nb_{1}O_{D5}}$	153 (1)	151 (1)
$\mathrm{Nb_{1}O_{D1}W_{1}}$	116 (1)	123 (2)	$\mathrm{O_{G2}Nb_{2}O_{D3}}$	100 (1)	103 (1)	$\mathrm{O_{A}W_{2}O_{E4}}$	77 (1)	72 (1)	$\mathrm{O_{B}Nb_{2}O_{D3}}$	156 (1)	152 (1)
$\mathrm{Nb_{2}O_{D2}W_{1}}$	117 (2)	121 (2)	$\mathrm{O_{G2}Nb_{2}O_{D6}}$	104 (1)	105 (2)	$\mathrm{O_{A}W_{3}O_{D3}}$	79 (1)	77 (1)	$\mathrm{O_{D2}Nb_{2}O_{D6}}$	152 (1)	150 (1)
$\mathrm{Nb_{2}O_{D3}W_{3}}$	112 (1)	119 (1)	$\mathrm{O_{H1}W_{1}O_{D1}}$	101 (2)	111 (2)	$\mathrm{O_{A}W_{3}O_{E1}}$	78 (1)	76 (1)	$\mathrm{O_{D1}W_{1}O_{E1}}$	152 (1)	151 (1)
$\mathrm{Nb_{1}O_{D4}W_{4}}$	117 1)	115 (1)	$\mathrm{O_{H1}W_{1}O_{D2}}$	104 (1)	113 (2)	$\mathrm{O_{A}W_{3}O_{E3}}$	73 (1)	70 (2)	$\mathrm{O_{D2}W_{1}O_{E2}}$	153 (1)	151 (1)
$\mathrm{Nb_{1}O_{D5}W_{2}}$	119 (1)	113 (1)	$\mathrm{O_{H1}W_{1}O_{E1}}$	107 (2)	97 (2)	$\mathrm{O_{A}W_{3}O_{F}}$	75 (1)	76 (1)	$\mathrm{O_{D5}W_{2}O_{E3}}$	149 (1)	151 (2)
$\mathrm{Nb_{2}O_{D6}W_{2}}$	116 (2)	116 (2)	$\mathrm{O_{H1}W_{1}O_{E2}}$	103 (2)	95 (2)	$\mathrm{O_{A}W_{4}O_{D4}}$	77 (1)	78 (1)	$\mathrm{O_{D6}W_{2}O_{E4}}$	154 (1)	151 (2)
$\mathrm{W_{1}O_{E1}W_{3}}$	119 (2)	118 (2)	$\mathrm{O_{H2}W_{2}O_{D5}}$	107 (2)	99 (2)	$\mathrm{O_{A}W_{4}O_{E2}}$	78 (1)	78 (1)	$\mathrm{O_{D3}W_{3}O_{F}}$	154 (1)	152 (1)
$\mathrm{W_{1}O_{E2}W_{4}}$	117 (2)	113 (2)	$\mathrm{O_{H2}W_{2}O_{D6}}$	105 (2)	102 (2)	$\mathrm{O_{A}W_{4}O_{E4}}$	72 (1)	77 (1)	$\mathrm{O_{E1}W_{3}O_{E3}}$	151 (1)	146 (1)
$\mathrm{W_{2}O_{E3}W_{3}}$	121 (2)	126 (3)	$\mathrm{O_{H2}W_{2}O_{E3}}$	104 (2)	110 (2)	$\mathrm{O_{A}W_{4}O_{F}}$	77 (1)	74 (1)	$\mathrm{O_{E2}W_{4}O_{E4}}$	150 (1)	155 (1)
						$\mathrm{O_{B}Nb_{1}O_{D1}}$	89 (1)	85 (1)	$\mathrm{O_{D4}W_{4}O_{F}}$	153 (1)	152 (1)
						$\mathrm{O_{B}Nb_{1}O_{D5}}$	85 (1)	90 (1)			

[a] The numbers in parentheses are the estimated standard deviations in the last significant digit. [b] Atoms are labeled in agreement with Tables II and S1[11] and Figures 2 and 3. [c] $C_{g1,2}$ and $C_{g5,6}$ are used to represent the midpoints of the C_1–C_2 and C_5–C_6 olefinic cyclooctadiene bonds, respectively. [d] Atoms labeled with primes are related to those without primes by the crystallographic inversions centers at (0, 0, 0) and ($^1/_2$, $^1/_2$, $^1/_2$) of the unit cell for anions I and II, respectively.

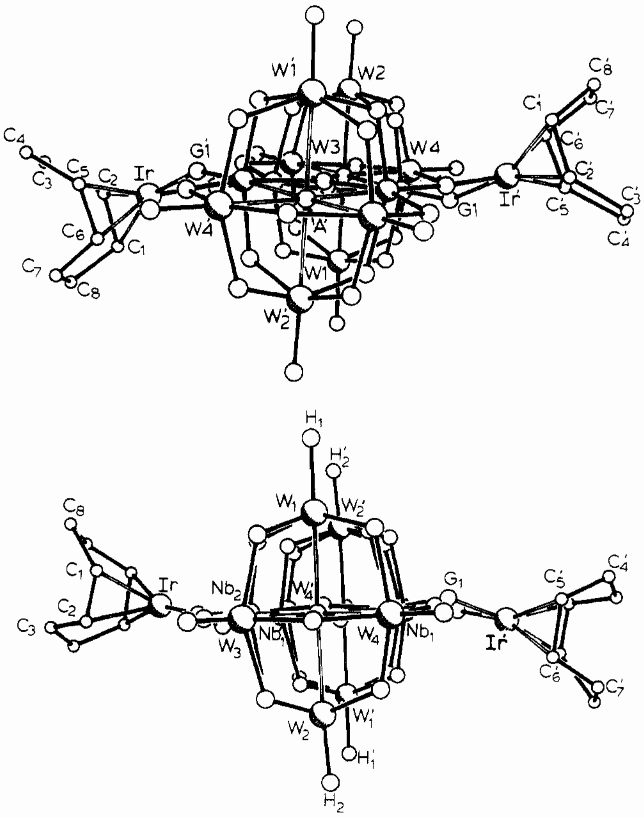

Figure 3. Perspective drawings of the two crystallographically independent $\{[(C_8H_{12})Ir]_2H(Nb_2W_4O_{19})_2\}^{5-}$ anions in crystalline $\{[(C_8H_{12})Ir]_2H(Nb_2W_4O_{19})_2\}[(n\text{-}C_4H_9)_4N]_5$: (a, top) anion I; (b, bottom) anion II. Both views are nearly parallel to the planar Ir coordination groups and perpendicular to the Ir → Ir' vector. See Figure 2 caption for the labeling scheme.

Å less than the 2.80 Å van der Waals diameter[20] of oxygen and the two independent O_{G1}'–Ir–O_{G2} angles of 84 (1) and 87 (1)° are both ≥3° less than the idealized 90° square-planar value even though the two oxygen atoms bonded to each Ir belong to different cis-$Nb_2W_4O_{19}^{4-}$ anions. Furthermore, the 2.84 (3) and 2.72 (3) Å $O_B\cdots O_B'$ separations for anion I and anion II, respectively, are fairly short and reminiscent of the 2.6–2.8-Å O···O separations between hydrogen-bonded polyoxoanions in crystalline $[H_3V_{10}O_{28}][P(C_6H_5)_4]_3\cdot 4CH_3CN$.[21,22]

Placing the unique proton of each dimeric anion between the basic[23] O_B and O_B' oxygen atoms at (or near) the crystallographic inversion centers would produce a hydrogen bond[24] between the two $Nb_2W_4O_{19}^{4-}$ moieties of each dimeric anion in **3** and could explain the structural anomalies noted above. Positioning both protons *on* their respective inversion centers as has been done in Figure 2 produces a symmetrical hydrogen bond between each O_B/O_B' pair with an average $O_B\cdots H$ distance of 1.39 Å (4, 3, 3, 2) and average Nb–O_B–Nb and Nb–O_B–H angles of 111 (2, 1, 1, 2) and 123° (2, 5, 7, 4), respectively. With the sum of the bond angles around O_B being 358.8° for anion I and 357.4° for anion II, a symmetrical hydrogen bond would seem to imply something much closer to sp^2 hybridization for the O_B atoms in **3** rather than the sp^3 hybridization observed for protonated and hydrogen-bonded doubly bridging oxygen atoms in $[H_3V_{10}O_{28}][P(C_6H_5)_4]_3\cdot 4CH_3CN$[21] and methylated doubly bridging oxygens in $[(Nb_2W_4O_{19})CH_3][(n\text{-}C_4H_9)_4N]_3$.[23] Moving the protons off the crystallographic inversion centers toward a given O_B or O_B' atom would produce an unsymmetrical hydrogen bond between pairs of cis-$Nb_2W_4O_{19}^{4-}$ anions and a situation where one of these anions is formally protonated and the other is not. Should this be the actual case, one might anticipate statistical disordering of the protonating hydrogen between these two oxygens in the solid state and an average structure like the one observed.

The unprotonated $\{[(C_8H_{12})Ir)_2(Nb_2W_4O_{19})_2\}^{6-}$ dimer with the same atom connectivity shown in Figure 2 might be expected to have a reasonably large number of closely related low-energy conformations, since the rigid cis-$Nb_2W_4O_{19}^{4-}$ anions and square-planar $(C_8H_{12})Ir^+$ cations might easily rotate with respect to each other through rotations about metal–O_G bonds and adjustment of the Ir–O_G–Nb bond angles. Given this flexibility, these conformations would undoubtedly have quite normal square-planar coordination for Ir(I) (i.e. O–Ir–O angles ≥90°) and intramolecular contacts between O_G oxygen atoms of the two $Nb_2W_4O_{19}^{4-}$ moieties that are not less than the 2.80-Å van der Waals diameter[20] of oxygen. The most favorable of these low-energy conformations would undoubtedly be the "fully extended" D_{2h} conformation in which both Ir coordination squares and both Nb_2W_4 squares were all coplanar and the Nb–O_G–Ir angles all close to 180°. Protonation of such a dimeric $\{[(C_8H_{12})Ir]_2(Nb_2W_4O_{19})_2\}^{6-}$ anion at one of its two most basic[23] (O_B or O_B') sites and subsequent hydrogen-bond formation with the second basic site would cause the two $Nb_2W_4O_{19}^{4-}$ anions to move closer together. Since the midpoint of the line connecting the terminal O_G atoms within a given $Nb_2W_4O_{19}^{4-}$ anion is slightly farther from the central O_A atom than is the doubly bridging O_B oxygen,[25] the $O_{G1}\cdots O_{G2}'$ and $O_{G1}'\cdots O_{G2}$ contacts would become critically short (<2.80 Å) before a strong hydrogen bond could be formed between O_B and O_B' if the two $Nb_2W_4O_{19}^{4-}$ anions were to approach each other along the $O_B \rightarrow O_B'$ vector while maintaining D_{2h} symmetry. The O_G oxygens can, however, maintain reasonable nonbonded separations if, as the two O_B oxygens approach each other from the fully extended D_{2h} planar conformation to form the hydrogen bond, either the two $Nb_2W_4O_{19}^{4-}$ anions rotate with respect to each other about the $O_B \rightarrow O_B'$ vector or they both rotate about their $O_{G1} \rightarrow O_{G2}$ (or $O_{G1}' \rightarrow O_{G2}'$) vectors to produce a step between the Nb_2W_2 squares. The latter motion will permit more linear Nb–O_G–Ir angles and will therefore probably be preferred. This type of O_B/O_B' approach does not require rotation of the $(C_8H_{12})Ir(O_G)_2$ squares out of the $4O_G$ mean plane, but such a rotation does allow the Ir–O_G–Nb angles to be optimized. The observed geometry for the non-hydrogen atoms of **3** therefore seems to represent the best compromise for the various structural constraints, i.e., two rigid $Nb_2W_4O_{19}^{4-}$ anions bridged by two square-planar $(C_8H_{12})Ir^+$ cations and a single proton with normal O···O contacts and a hydrogen bond between the two most basic oxygens.

Solution ^{17}O NMR spectroscopic data indicate that the structure observed for the anion of **3** in the solid state is maintained in nitromethane solution (see Figure 4). Assuming D_{2h} symmetry on the NMR time scale, the anion of **3** contains nine types of symmetry-equivalent oxygens: one type of ONb_2W_4 oxygen (two O_A oxygens), one type of ONb_2H oxygen (two O_B oxygens), two types of OW_2 oxygens (eight O_C oxygens, two O_D oxygens), two types of ONbW oxygens (eight O_E oxygens, four O_F oxygens), one type of ONbIr oxygen (four O_G oxygens), and two types of OW oxygens (four O_H oxygens, four O_I oxygens). The resonances observed at δ 727, 457, and 388 are assigned to OW, ONbW, and OW_2 oxygens, respectively, since these types of oxygens in the related complexes $[(CH_3)_5C_5]Rh(Nb_2W_4O_{19})^{2-}$, $(OC)_3Mn(Nb_2W_4O_{19})^{3-}$, and $(OC)_3Re(Nb_2W_4O_{19})^{3-}$ are known to have about the same ^{17}O NMR chemical shifts.[8,26] The ONb_2W_4

---

[20] Pauling, L. *The Nature of the Chemical Bond*, 3rd ed.; Cornell University Press: Ithaca, NY, 1960; p 260.

[21] Day, V. W.; Klemperer, W. G.; Maltbie, D. J. *J. Am. Chem. Soc.* **1987**, *109*, 2991.

[22] For other hydrogen-bonded polyoxoanion dimers, see: Lee, U.; Sasaki, Y. *Chem. Lett.* **1984**, 1297.

[23] The oxygens bridging the two Nb atoms in $Nb_2W_4O_{19}^{4-}$ are the most basic surface oxygen atoms in the anion: Day, V. W.; Klemperer, W. G.; Schwartz, C. *J. Am. Chem. Soc.* **1987**, *109*, 6030.

[24] For discussions of related hydrogen bonds between metal hydroxide centers, see: (a) Ardon, M.; Bino, A. *Struct. Bonding* **1987**, *65*, 1. (b) Springborg, J. *Adv. Inorg. Chem.* **1988**, *32*, 55.

[25] This relationship between doubly bridging and terminal oxygens in hexametalate structures is graphically illustrated in Schemes I and II of ref 8.

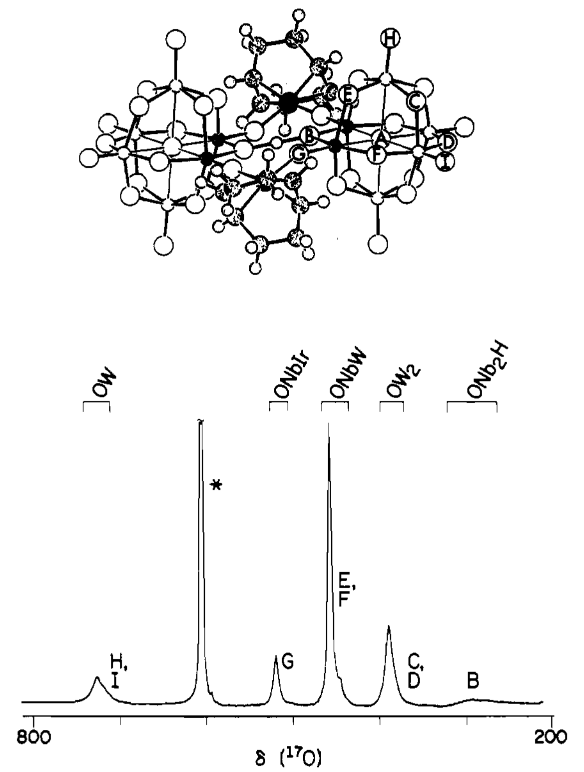

Figure 4. Top: SCHAKAL drawing of the $\{[(C_8H_{12})Ir]_2H(Nb_2W_4O_{19})_2\}^{5-}$ anion. Oxygen atoms are represented by large open spheres, iridium atoms by large filled spheres, tungsten atoms by small open spheres, niobium atoms by small filled spheres, hydrogen atoms by small shaded spheres, and carbon atoms by medium-sized shaded spheres. One member of each set of symmetry-equivalent oxygen atoms is labeled, assuming D_{2h} symmetry. Bottom: ^{17}O NMR spectrum of $\{[(C_8H_{12})Ir]_2H(Nb_2W_4O_{19})_2\}[(n\text{-}C_4H_9)_4N]_5$ in CH_3NO_2. See text for assignments and Experimental Section for numerical data and experimental parameters. The resonance marked with an asterisk (*) is due to the solvent.

oxygens (O_A) are not observed due to the insufficient ^{17}O content obtained during ^{17}O enrichment of the $Nb_2W_4O_{19}{}^{4-}$ ligand.[2b] There remain, therefore, two resonances to be assigned to the two remaining types of oxygen, O_B and O_G. Since binding of a cation to a $Nb_2W_4O_{19}{}^{4-}$ oxygen is expected to displace its chemical shift upfield,[27] the δ 520 resonance is assigned to the ONbIr oxygens, not the ONb_2H oxygens: $\delta(ONb) = 752$ and $\delta(ONb_2) = 491$ in $Nb_2W_4O_{19}{}^{4-}$.[8] By default, the δ 293 resonance is assigned to the ONb_2H oxygen, O_B. This oxygen has a chemical shift value upfield relative to the δ 491 chemical shift of the unprotonated ONb_2 oxygen in $Nb_2W_4O_{19}{}^{4-}$ but downfield relative to the δ 187 chemical shift of the ONb_2H oxygen in $Nb_2W_4O_{19}H^{3-}$[23] in part because the proton in the anion of **3** is shared by two ONb_2 oxygens.

$[(C_8H_{12})Ir(P_3O_9)][(n\text{-}C_4H_9)_4N]_2$ (4). Reaction of $[(C_8H_{12})Ir(NCCH_3)_2]PF_6$ with $P_3O_9[(n\text{-}C_4H_9)_4N]_3$ according to eq 3 in CH_2Cl_2 followed by crystallization of the crude product from acetone/diethyl ether yields $[(C_8H_{12})Ir(P_3O_9)][(n\text{-}C_4H_9)_4N]_2$ (**4**) in >65% yield.

$$(C_8H_{12})Ir(NCCH_3)_2{}^+ + P_3O_9{}^{3-} \rightarrow (C_8H_{12})Ir(P_3O_9)^{2-} + 2CH_3CN \quad (3)$$

X-ray structural analysis revealed that single crystals of $[(C_8H_{12})Ir(P_3O_9)][(n\text{-}C_4H_9)_4N]_2$ (**4**) are composed of discrete $(n\text{-}C_4H_9)_4N^+$ cations (Figure S2[11]) and $[(C_8H_{12})Ir(P_3O_9)]^{2-}$ anions (Figure 5). Final atomic coordinates and thermal parameters for non-hydrogen atoms of **4** are listed with estimated standard deviations in Tables IV and S3.[11] Bond lengths and angles in the $[(C_8H_{12})Ir(P_3O_9)]^{2-}$ anion and the $(n\text{-}C_4H_9)_4N^+$ cations of **4** are given in Tables V and S4,[11] respectively.

Table IV. Fractional Atomic Coordinates for Non-Hydrogen Atoms in Crystalline $[(C_8H_{12})Ir(P_3O_9)][(n\text{-}C_4H_9)_4N]_2$ (**4**)[a]

atom type[b]	10^3x	10^3y	10^3z	B,[c] Å
		Anion		
Ir	−106.9 (2)	150.7 (1)	98.3 (1)	11.6 (1)
P_1	26.0 (7)	390.4 (5)	124.7 (2)	8.0 (3)
P_2	−156.8 (11)	316.2 (5)	164.7 (3)	8.0 (4)
P_3	−221.4 (10)	381.0 (5)	83.5 (2)	8.0 (4)
O_1	65.8 (17)	293.7 (11)	110.5 (5)	9.3 (7)
O_2	−152.4 (15)	207.7 (11)	152.7 (5)	8.1 (6)
O_3	−211.8 (18)	278.3 (10)	67.6 (5)	10.2 (8)
O_{t1}	110.1 (17)	475.8 (12)	136.5 (7)	10.4 (8)
O_{t2}	−195.6 (19)	340.1 (13)	202.3 (5)	12.3 (8)
O_{t3}	−300.1 (18)	455.9 (13)	62.4 (5)	9.5 (8)
O_{12}	−36.2 (18)	370.9 (12)	162.6 (5)	7.7 (7)
O_{13}	−90.6 (16)	426.7 (11)	91.9 (5)	7.6 (7)
O_{23}	−247.5 (15)	370.6 (12)	129.5 (6)	8.1 (7)
C_1	−38 (3)	107 (2)	48 (1)	11 (2)
C_2	−175 (4)	57 (2)	41 (1)	18 (2)
C_3	−210 (5)	−46 (3)	51 (2)	21 (2)
C_4	−171 (1)	−33 (7)	98 (2)	30 (4)
C_5	−112 (3)	19 (2)	121 (1)	12 (2)
C_6	−4 (5)	21 (4)	123 (1)	23 (3)
C_7	85 (5)	−12 (4)	95 (2)	24 (3)
C_8	73 (4)	68 (5)	68 (2)	26 (4)
		Cation 1		
N	5 (2)	−141 (1)	−280 (1)	8 (1)
C_{a1}	78 (2)	−229 (2)	−288 (1)	7 (1)
C_{a2}	72 (2)	−43 (2)	−268 (1)	7 (1)
C_{a3}	−62 (2)	−176 (2)	−247 (1)	8 (1)
C_{a4}	−95 (2)	−112 (2)	−319 (1)	8 (1)
C_{b1}	157 (2)	−204 (2)	−320 (1)	9 (1)
C_{b2}	181 (4)	−60 (3)	−233 (1)	9 (1)
C_{b3}	−151 (3)	−96 (2)	−233 (1)	10 (1)
C_{b4}	−175 (3)	−200 (2)	−331 (1)	11 (1)
C_{g1}	244 (3)	−299 (2)	−314 (1)	13 (1)
C_{g2}	239 (3)	46 (2)	−226 (1)	11 (1)
C_{g3}	−226 (3)	−165 (2)	−206 (1)	14 (1)
C_{g4}	−268 (3)	−155 (2)	−366 (1)	14 (1)
C_{d1}	305 (5)	−285 (4)	−324 (2)	26 (2)
C_{d2}	362 (3)	30 (2)	−195 (1)	14 (1)
C_{d3}	−310 (5)	−101 (3)	−196 (2)	23 (2)
C_{d4}	−355 (4)	−224 (3)	−382 (1)	19 (2)
		Cation 2		
N	334 (2)	105 (1)	558 (1)	8 (1)
C_{a1}	417 (2)	190 (2)	549 (1)	9 (1)
C_{a2}	334 (2)	85 (2)	605 (1)	8 (1)
C_{a3}	392 (2)	12 (2)	542 (1)	8 (1)
C_{a4}	200 (3)	120 (2)	540 (1)	8 (1)
C_{b1}	379 (4)	294 (3)	566 (1)	14 (1)
C_{b2}	470 (3)	71 (2)	630 (1)	12 (1)
C_{b3}	319 (3)	−88 (2)	549 (1)	10 (1)
C_{b4}	183 (2)	140 (2)	494 (1)	9 (1)
C_{g1}	479 (4)	373 (3)	555 (1)	16 (1)
C_{g2}[d]	469 (5)	89 (5)	680 (2)	9 (1)
C_{g2}'[d]	466 (5)	19 (4)	682 (2)	7 (1)
C_{g3}	393 (3)	−172 (2)	529 (1)	11 (1)
C_{g4}	42 (2)	148 (2)	482 (1)	10 (1)
C_{d1}	455 (4)	470 (3)	576 (1)	18 (1)
C_{d3}	338 (3)	−268 (2)	539 (1)	14 (1)
C_{d4}	4 (3)	179 (2)	437 (1)	12 (1)

[a] The numbers in parentheses are the estimated standard deviations in the last significant digit. [b] Atoms are labeled in agreement with Figures 5 and S2.[11] [c] Isotropic thermal parameter; for atoms of the anion, this is one-third of the trace of the orthogonalized $\mathbf{B}_{ij}$ tensor; for atoms of the cations, it is the refined value of the isotropic thermal parameter. [d] Methylene carbon atom C_{g2} of cation 2 is statistically disordered between two sites in the lattice, C_{g2} and C_{g2}'; terminal methyl carbon C_{d2} of cation 2 could not be located from difference Fourier syntheses.

The iridium(I) centers in **4** achieve an 18-electron configuration through square-pyramidal coordination by two olefinic C=C bonds of a cyclooctadiene (COD) ligand plus three terminal oxygens of a trimetaphosphate ligand. Two cis basal sites of the

---

(26) Besecker, C. J.; Day, V. W.; Klemperer, W. G.; Thompson, M. R. *Inorg. Chem.* **1985**, *24*, 44.

(27) Day, V. W.; Klemperer, W. G. *Science (Washington, D.C.)* **1985**, *228*, 533.

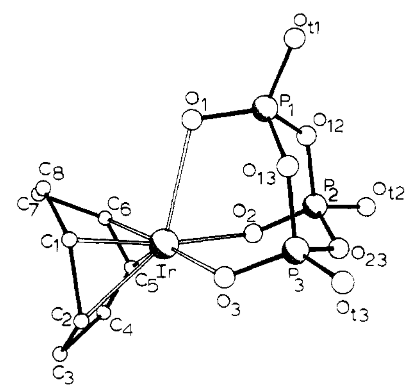

Figure 5. Perspective drawing of the $[(C_8H_{12})Ir(P_3O_9)]^{2-}$ anion in crystalline $[(C_8H_{12})Ir(P_3O_9)][(n\text{-}C_4H_9)_4N]_2$. The iridium and phosphorus atoms are represented by large- and medium-sized shaded spheres, respectively. Oxygen and carbon atoms are represented by medium-sized and small open spheres, respectively. Hydrogen atoms are not shown.

square pyramid are occupied by the two C=C bonds, and the remaining two cis basal sites, by oxygen atoms O_2 and O_3 of the $P_3O_9^{3-}$ ligand; the apical site is occupied by oxygen atom O_1 of the same trimetaphosphate group. The midpoints of the two olefinic C=C bonds ($C_{1,2}$ and $C_{5,6}$) and the two basally coordinated $P_3O_9^{3-}$ oxygen atoms (O_2 and O_3) are coplanar[28a] to within 0.009 Å. The iridium atom is displaced by 0.275 Å from this basal plane toward O_1. The least-squares mean plane[28b] containing Ir, P_1, O_1, O_{t1}, and O_{23} forms a dihedral angle of 88° with the basal mean plane. Within the basal plane, Ir–C bond distances and Ir–O bond distances have average values of 2.13 (4, 11, 21, 4)[19] and 2.18 Å (2, 3, 3, 2), respectively. The apical Ir–O_1 bond length is 2.70 (2) Å.

Table V. Bond Lengths (Å) and Angles (deg) in the $[(C_8H_{12})Ir(P_3O_9)]^{2-}$ Anion of Crystalline $[(C_8H_{12})Ir(P_3O_9)][(n\text{-}C_4H_9)_4N]_2$ (**4**)[a]

type[b]	value	type[b]	value
	Bond Lengths		
Ir–O_2	2.15 (2)	Ir–O_1	2.70 (2)
Ir–O_3	2.21 (2)	Ir–$C_{1,2}$[c]	2.05
Ir–C_1	2.11 (4)	Ir–$C_{5,6}$[c]	1.95
Ir–C_2	2.32 (4)	C_1–C_2	1.66 (6)
Ir–C_5	1.92 (3)	C_5–C_6	1.22 (6)
Ir–C_6	2.15 (2)	C_2–C_3	1.48 (6)
P_1–O_1	1.48 (2)	C_3–C_4	1.58 (9)
P_2–O_2	1.50 (2)	C_4–C_5	1.15 (9)
P_3–O_3	1.48 (2)	C_6–C_7	1.57 (8)
P_1–O_{t1}	1.49 (2)	C_7–C_8	1.39 (9)
P_2–O_{t2}	1.47 (2)	C_1–C_8	1.41 (6)
P_3–O_{t3}	1.43 (2)	P_2–O_{23}	1.59 (2)
P_1–O_{12}	1.61 (2)	P_3–O_{13}	1.57 (2)
P_1–O_{13}	1.63 (2)	P_3–O_{23}	1.66 (2)
P_2–O_{12}	1.56 (2)		
	Bond Angles		
O_1IrO_2	84.7 (6)	C_3C_2Ir	111 (3)
O_1IrO_3	80.8 (6)	C_4C_5Ir	109 (5)
$O_1IrC_{1,2}$[c]	109.1	C_7C_6Ir	111 (3)
$O_1IrC_{5,6}$[c]	115.1	C_2C_1Ir	75 (2)
O_2IrO_3	86.6 (6)	C_1C_2Ir	61 (2)
$C_{1,2}IrC_{5,6}$[c]	85.1	C_6C_5Ir	83 (3)
$O_2IrC_{5,6}$[c]	93.5	C_5C_6Ir	62 (3)
$O_3IrC_{1,2}$[c]	90.8	$C_8C_1C_2$	130 (3)
$O_2IrC_{1,2}$[c]	165.4	$C_1C_2C_3$	129 (3)
$O_3IrC_{5,6}$[c]	164.1	$C_4C_5C_6$	120 (6)
O_1IrC_1	87 (1)	$C_5C_6C_7$	136 (4)
O_1IrC_6	100 (1)	$C_2C_3C_4$	95 (4)
O_1IrC_2	129 (1)	$C_3C_4C_5$	140 (8)
O_1IrC_5	131 (1)	$C_6C_7C_8$	101 (4)
O_2IrC_6	99 (1)	$C_7C_8C_1$	124 (5)
O_3IrC_1	94 (1)	$O_1P_1O_{t1}$	122 (1)
O_2IrC_5	87 (1)	$O_2P_2O_{t2}$	118 (1)
O_3IrC_2	88 (1)	$O_3P_3O_{t3}$	123 (1)
O_2IrC_1	172 (1)	$O_1P_1O_{12}$	109 (1)
O_3IrC_6	174 (1)	$O_1P_1O_{13}$	107 (1)
O_2IrC_2	145 (1)	$O_2P_2O_{12}$	111 (1)
O_3IrC_5	147 (1)	$O_2P_2O_{23}$	107 (1)
IrO_1P_1	114 (1)	$O_3P_3O_{13}$	107 (1)
IrO_2P_2	127 (1)	$O_3P_3O_{23}$	108 (1)
IrO_3P_3	127 (1)	$O_{t1}P_1O_{12}$	105 (1)
$P_1O_{12}P_2$	129 (1)	$O_{t1}P_1O_{13}$	111 (1)
$P_1O_{13}P_3$	128 (1)	$O_{t2}P_2O_{12}$	111 (1)
$P_2O_{23}P_3$	123 (1)	$O_{t2}P_2O_{23}$	107 (1)
C_8C_1Ir	98 (3)	$O_{t3}P_3O_{13}$	107 (1)
		$O_{t3}P_3O_{23}$	109 (1)
		$O_{12}P_1O_{13}$	100 (1)
		$O_{12}P_2O_{23}$	101 (1)
		$O_{13}P_3O_{23}$	101 (1)

[a] The numbers in parentheses are the estimated standard deviation in the last significant digit. [b] Atoms are labeled in agreement with Tables IV and S3[11] and Figure 5. [c] $C_{1,2}$ and $C_{5,6}$ refer to the midpoints of the C_1–C_2 and C_5–C_6 olefinic bonds, respectively.

Generally speaking, five-coordinate (cyclooctadiene)iridium(I) complexes tend to adopt trigonal-bipyramidal coordination geometry with the bidentate COD ligand spanning axial and equatorial positions, as observed in complexes such as $(C_8H_{12})[(C_6H_5)(CH_3)_2P]_2(CH_3)Ir$,[29] $(C_8H_{12})[(C_6H_5)_2P(CH_2)_2P(C_6H_5)_2](CH_3)Ir$,[30] $(C_8H_{12})[(C_6H_5)_2P(CH_2)_3P(C_6H_5)_2](CH_3)Ir$,[31] (C_8H_{12})[2,3-(isopropylidenedioxy)-1,4-bis(diphenylphosphino)butane]ClIr,[32] (C_8H_{12})[(2*R*,3*R*)-2,3-(isopropylidenedioxy)-1,4-bis(5*H*-dibenzophosphol-5-yl)butane]ClIr,[33] $(C_8H_{12})Ir[P(OC_6H_4CH_3)(OCH_6H_4CH_3)_2][P(OCH_2)CCH_3]$,[34] $\{(C_8H_{12})[P(C_6H_5)_3]$(4,4′,5,5′-tetracyano-2,2′-biimidazolyl)Ir$\}^-$,[35] and $(C_8H_{12})_2(SnCl_3)Ir$.[36] To the best of our knowledge, only one example of a square-pyramidal, five-coordinate (cyclooctadiene)iridium(I) complex has been reported, namely, the carbon-bonded acetylacetonate complex (C_8H_{12})(acac)(phen)Ir, phen = phenanthroline.[37] Here, the basal sites are occupied by the N atoms of the phenanthroline ligand and the C=C bonds of the COD ligand, and the acac carbon occupies the apical site. The coordination geometry is quite similar to that observed in **4**. The olefinic Ir–C and phen Ir–N bond lengths average 2.127 (6, 14, 19, 4)[19] and 2.104 Å (5, 19, 19, 2), respectively; the apical Ir–C bond is longer at 2.420 (6) Å. The question of which physical factors are responsible for adoption of square-pyramidal as opposed to trigonal-bipyramidal geometry in d^8 transition-metal complexes has not been addressed in detailed theoretical studies of five-coordinate transition-metal complexes.[38,39]

NMR spectroscopic measurements indicate that the $(C_8H_{12})Ir(P_3O_9)^{2-}$ anion is fluxional in solution. The square-pyramidal structure shown in Figure 5 contains two symmetry-nonequivalent types of phosphorus atoms and two symmetry-

---

(28) The least-squares mean planes for the following groups of atoms in **4** are defined by the equation: $ax + by + cz = d$, where x, y, and z are orthogonal coordinates measured along $\vec{a}$, $\vec{b}$, and $\vec{c}^*$, respectively, of the crystal system. (a) $C_{1,2}$,[18] $C_{5,6}$,[18] O_2, and O_3 (coplanar to within 0.009 Å): $a = -0.904$, $b = -0.422$, $c = 0.066$, $d = 0.741$. (b) Ir, P_1, O_1, O_{t1}, and O_{23} (coplanar to within 0.05 Å): $a = 0.251$, $b = -0.311$, $c = 0.916$, $d = 2.326$.

(29) Churchill, M. R.; Bezman, S. A. *Inorg. Chem.* **1972**, *11*, 2243.

(30) Churchill, M. R.; Bezman, S. A. *Inorg. Chem.* **1973**, *12*, 260.

(31) Churchill, M. R.; Bezman, S. A. *Inorg. Chem.* **1973**, *12*, 531.

(32) Brunie, S.; Mazan, J.; Langlois, N.; Kagan, H. B. *J. Organomet. Chem.* **1976**, *114*, 225.

(33) Hayashi, T.; Tanaka, M.; Ogata, I.; Kodama, T.; Takahashi, T.; Uchida, Y.; Uchida, T. *Bull. Chem. Soc. Jpn.* **1983**, *56*, 1780.

(34) Laing, M.; Nolte, M. J.; Singleton, E.; Van Der Stok, E. *J. Organomet. Chem.* **1978**, *146*, 77.

(35) Rasmussen, P. G.; Bailey, O. H.; Bayón, J. C.; Butler, W. M. *Inorg. Chem.* **1984**, *23*, 343.

(36) Porta, P.; Powell, H. M.; Mawby, R. J.; Venanzi, L. M. *J. Chem. Soc. A* **1967**, 455.

(37) Oro, L. A.; Carmona, D.; Esternelas, M. A.; Foces-Foces, C.; Cano, F. H. *J. Organomet. Chem.* **1983**, *258*, 357.

(38) Rossi, A. R.; Hoffmann, R. *Inorg. Chem.* **1975**, *14*, 365.

(39) Albright, T. A.; Burdett, J. K.; Whangbo, M.-H. *Orbital Interactions in Chemistry*; Wiley: New York, 1985; Chapter 17.

Scheme II

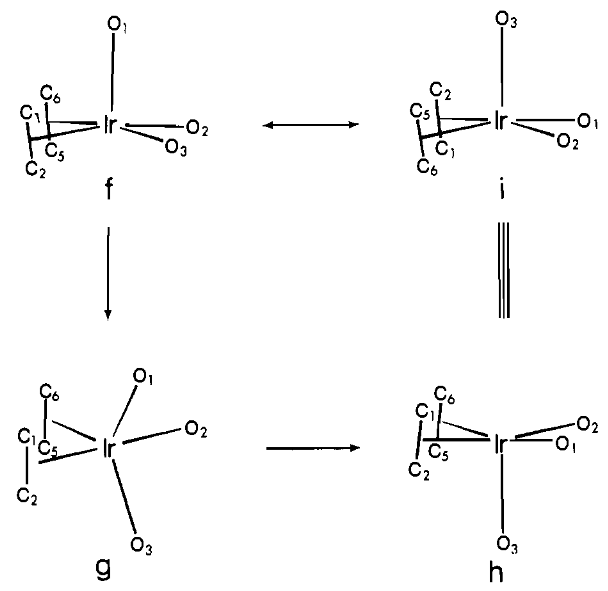

nonequivalent types of cyclooctadiene methine groups. NMR spectra of compound **4** in CH_2Cl_2 measured at ambient temperature, however, display only one phosphorus resonance, one methine carbon resonance, and one methine hydrogen resonance. When the solution temperature is lowered to −75 °C, the single ^{31}P NMR resonance shows no line broadening. Since mixtures of the cyclooctadieneiridium complex $(C_8H_{12})Ir(P_3O_9)^{2-}$ and the norbornadienerhodium complex $(C_7H_8)Rh(P_3O_9)^{2-}$ [2b] show two separate, single ^{31}P NMR resonances arising from the individual complexes, indicating no rapid trimetaphosphate exchange, the exchange process responsible for averaging phosphorus and methine environments in $(C_8H_{12})Ir(P_3O_9)^{2-}$ is presumed to be intramolecular. The equivalence of methine and of phosphorus environments in $(C_8H_{12})Ir(P_3O_9)^{2-}$ on the NMR time scale can be accounted for by rapid intramolecular rearrangement along the Berry pseudorotation[40] pathway indicated in Scheme II. The intermediate configuration, g, is trigonal bipyramidal with the cyclooctadiene ligand spanning axial and equatorial sites.

Stability Studies. Acetonitrile was selected as a good σ-donor ligand to determine the relative ease with which ligands can be displaced from iridium(I) in complexes **1**, **3**, and **4**. Treatment of compound **1** in CD_3NO_2 with 50 equiv of CD_3CN/mol of iridium resulted in complete degradation of the complex according to ^1H NMR spectroscopy (see Experimental Section). Under the same conditions, compound **3** showed no evidence of degradation, but addition of 250 equiv of CD_3CN/mol of iridium caused about 20% decomposition. Compound **4**, however, showed no evidence of degradation upon addition of 250 equiv of CD_3CN. These results give the order of increasing stability $[(C_8H_{12})Ir]_5(Nb_2W_4O_{19})_2^{3-} < [(C_8H_{12})Ir]_2H(Nb_2W_4O_{19})_2^{5-} < (C_8H_{12})Ir(P_3O_9)^{2-}$. This sequence cannot be interpreted solely in terms of the instability of coordinatively unsaturated square-planar Ir(I) relative to saturated square-pyramidal Ir(I), since $(C_8H_{12})Ir(C_5H_7O_2)$, $C_5H_7O_2$ = acetylacetonate, is stable toward 250 equiv of CD_3CN in CD_3NO_2 solution. Ligand basicity thus appears to be an important factor.

Acknowledgment. W.G.K. acknowledges the National Science Foundation for support of this research. We are grateful to Dr. Egbert Keller for providing a copy of his SCHAKAL program.

Supplementary Material Available: Crystal structure reports for compounds **3**, $\{[(C_8H_{12})Ir]_2H(Nb_2W_4O_{19})_2\}[(n\text{-}C_4H_9)_4N]_5$, and **4**, $[(C_8H_{12})Ir(P_3O_9)][(n\text{-}C_4H_9)_4N]_2$, Tables S1–S4, containing anisotropic thermal parameters for the metal atoms of **3**, bond lengths and angles in the cations of **3** and **4**, and anisotropic thermal parameters for nonhydrogen atoms in the anion of **4**, and Figures S1 and S2, showing perspective drawings of the cations of **3** and **4** (24 pages); structure factor tables for the crystal structure analyses of **3** and **4** (31 pages). Ordering information is given on any current masthead page.

---

(40) Shapley, J. R.; Osborn, J. A. *Acc. Chem. Res.* **1973**, *6*, 305.

Contribution from the Department of Chemistry,
University of Illinois, Urbana, Illinois 61801

Polyoxoanion-Supported Metal Carbonyls: Synthesis and Characterization of $\{[(OC)_2Rh]_5(Nb_2W_4O_{19})_2\}^{3-}$, $\{[(OC)_2Rh]_3(Nb_2W_4O_{19})_2\}^{5-}$, $\{[(OC)_2Ir]_2H(Nb_2W_4O_{19})_2\}^{5-}$, and $[(OC)_2Ir(P_3O_9)]^{2-}$

W. G. Klemperer* and D. J. Main

Received August 2, 1989

The first polyoxyanion-supported rhodium and iridium carbonyl complexes have been prepared as $(n\text{-}C_4H_9)_4N^+$ or $[(C_6H_5)_3P]_2N^+$ salts and assigned structures similar to those of known rhodium and iridium diene complexes by using multinuclear (^{17}O, ^{13}C, ^{183}W, and/or ^{31}P) NMR and IR spectroscopy. Reaction of either $\{[(C_7H_8)Rh]_5(Nb_2W_4O_{19})_2\}[(n\text{-}C_4H_9)_4N]_3$ with CO in nitromethane solution or $Nb_2W_4O_{19}[(n\text{-}C_4H_9)_4N]_4$ with $[(OC)_2RhCl]_2$ in 1,2-dichloroethane solution yields crystalline $\{[(OC)_2Rh]_5(Nb_2W_4O_{19})_2\}[(n\text{-}C_4H_9)_4N]_3$ (**1**) in 75% yield. The anion of **1** has a structure derived from its (norbornadiene)rhodium precursor by replacement of each C_7H_8 ligand by two CO ligands: two octahedral $Nb_2W_4O_{19}^{4-}$ anions are linked together face-to-face by five $(OC)_2Rh^+$ units. Reaction of $Nb_2W_4O_{19}[(n\text{-}C_4H_9)_4N]_4$ with $[(OC)_2RhCl]_2$ in chloroform yields $\{[(OC)_2Rh]_3(Nb_2W_4O_{19})_2\}[(n\text{-}C_4H_9)_4N]_5$ (**2**) in 41% yield. The structure proposed for the anion of **2** is obtained by removing two $(OC)_2Rh^+$ units from the structure of the anion of **1**, specifically, those bonded to ONbW oxygens. Bubbling CO through a CH_3CN solution of $\{[(C_8H_{12})Ir]_2H(Nb_2W_4O_{19})_2\}[(n\text{-}C_4H_9)_4N]_5$ yields $\{[(OC)_2Ir]_2H(Nb_2W_4O_{19})_2\}[(n\text{-}C_4H_9)_4N]_5$ (**3**) in >80% yield. The anion of **3** is proposed to have a structure derived from the structure of its (cyclooctadiene)iridium precursor by replacement of each C_8H_{12} ligand with two CO ligands. In this structure, two octahedral $Nb_2W_4O_{19}^{4-}$ anions are linked together edge-to-edge by a proton and two $(OC)_2Ir^+$ cations. The trimetaphosphate complex $[(OC)_2Ir(P_3O_9)]\{[(C_6H_5)_3P]_2N\}_2$ (**4**) is prepared by substitution of cyclooctadiene ligands in $[(C_8H_{12})Ir(P_3O_9)]\{[(C_6H_5)_3P]_2N\}_2$ with CO ligands. As was the case with compounds **1** and **3**, the anion of **4** is proposed to have a structure derived from the diene precursor structure by replacement of each diene ligand with two CO ligands, yielding a square-pyramidal Ir(I) complex having two basal CO ligands and a $\kappa^3O\text{-}P_3O_9^{3-}$ ligand spanning two adjacent basal and the apical sites.

The chemistry of solid oxide supported rhodium and iridium carbonyl complexes has been studied in some detail.[1] In order to develop a similar chemistry of soluble organometallic oxide complexes, we have begun to investigate analogous polyoxo-